Aus der Medizinischen Klinik
mit Schwerpunkt Infektiologie und Pneumologie
der Medizinischen Fakultät Charité – Universitätsmedizin Berlin

DISSERTATION

Experimentelle Untersuchung einer neuartigen adjuvanten Therapie auf Immunglobulinbasis bei schwerer Lungenentzündung unter mechanischer Beatmung

Experimental investigation of a novel immunoglobulin-based adjuvant therapy for severe pneumonia under mechanical ventilation

zur Erlangung des akademischen Grades
Doctor medicinae (Dr. med.)

vorgelegt der Medizinischen Fakultät
Charité – Universitätsmedizin Berlin

von

Alexander Taylor
M.B. B.Chir. M.A. (Cantab)

aus Birmingham, Großbritannien

Datum der Promotion: 03.12.2021

Table of Contents

1. List of Figures and Tables

1.1. List of Figures

1.2. List of Tables

2. List of abbreviations

AM	alveolar macrophage
ARDS	acute respiratory distress syndrome
AST	aspartate transaminase
ATS	American Thoracic Society
BAL	bronchoalveolar lavage
BALF	bronchoalveolar lavage fluid
BTS	British Thoracic Society
BUN	blood urea nitrogen
C	compliance
C1q	complement component 1q
C3	complement component 3
C4	complement component 4
C5a	complement component 5a
C5b-C9	complement components 5b-9
C6	complement component 6
Ca^{2+}	calcium
CAP	community-acquired pneumonia
CCL2	chemokine (CC motif) ligand 2
CCL5	chemokine (CC motif) ligand 5
CIGMA	concentrated IgM for application
Cl^-	chloride
CRP	C-reactive protein
CXCL1	chemokine (CXC motif) ligand 1
CXCL3	chemokine (CXC motif) ligand 3

CXCL5	chemokine (CXC motif) ligand 5
CXCL10	chemokine (CXC motif) ligand 10
CXCR2	chemokine (CXC motif) receptor 2
DAMP	danger-associated molecular pattern
DM	dendritic cell
E	elastance
ELISA	enzyme-linked immunosorbent assay
EOS	eosinophil
FACS	fluorescence-activated cell sorting
FELASA	Federation of European Laboratory Animal Science Associations
FiO_2	fraction of inspired oxygen
GM-CSF	granulocyte-macrophage colony-stimulating factor
GRA	granulocyte
H&E	haemotoxylin and eosin
HCO_3^-	bicarbonate
HCT	haematocrit
HGB	haemoglobin
HMG CoA	3-hydroxy-3-methyl-glutaryl-coenzyme A
HMGB-1	high mobility group box-1
HR	heart rate
HVT	high tidal volume
I:E	inspiratory:expiratory ratio
ICU	intensive care unit
IDSA	Infectious Disease Society of America

IFN-α	interferon-α
IFN-β	interferon-β
IFN-γ	interferon-γ
IgA	immunoglobulin A
IgG	immunoglobulin G
IgM	immunoglobulin M
IL-1	interleukin-1
IL-1β	interleukin-1β
IL-1ra	interleukin-1 receptor antagonist
IL-6	interleukin-6
IL-10	interleukin-10
IL-12	interleukin-12
IM	inflammatory macrophage/monocyte
IQR	interquartile range
IRF-3	interferon regulatory factor-3
IRF-7	interferon regulatory factor-7
ITP	idiopathic thrombocytopenic purpura
IVIg	intravenous immunoglobulin
K^+	potassium
kg	kilogram
KGF	keratinocyte growth factor
LAGeSo	Landesamt für Gesundheit und Soziales
LH	lung homogenate
LPS	lipopolysaccharide
LVT	low tidal volume

LYM	lymphocyte
MAP	mean arterial pressure
MCH	mean corpuscular haemoglobin
MCHC	mean corpuscular haemoglobin concentration
MCV	mean corpuscular volume
MHC	major histocompatibility complex
ml	millilitre
MON	monocyte
MPO	myeloperoxidase
MPV	mean platelet volume
MSA	murine serum albumin
MV	mechanical ventilation
Na^+	sodium
NET	neutrophil extracellular trap
NF-κB	nuclear factor kappa-light-chain-enhancer of activated B cells
NLRP3	NACHT, LRR and PYD domains-containing protein 3
NV	non-ventilated
$PaCO_2$	partial pressure of carbon dioxide
PAMP	pathogen-associated molecular pattern
PaO	airway opening pressure
PaO_2	partial pressure of oxygen
PAS	Periodic-acid Schiff
PEEP	positive end-expiratory pressure
PMN	polymorphonuclear neutrophil
PNT	Pentaglobin

R	resistance
RBC	red blood cell
ROS	reactive oxygen species
S. pneumoniae	Streptococcus pneumoniae
SBE	standard base excess
sCAP	severe community-acquired pneumonia
SD	standard deviation
SEM	standard error of the mean
SpO_2	oxygen saturation
$stPaO_2$	standardized partial pressure of oxygen
TLR	Toll-like receptor
TNF-α	tumour necrosis factor-α
UK	United Kingdom
USA	United States of America
VAP	ventilator-associated pneumonia
VILI	ventilator-induced lung injury
VT	tidal volume
WBC	white blood cell

3. Summary

In its most devastating form, severe community-acquired pneumonia necessitates mechanical ventilation, a life-saving intervention to prevent death from respiratory failure. This in itself is not without risks and a well-recognized, unfortunate complication is ventilator-induced lung injury. Ventilator-induced lung injury is defined by the breakdown of the alveolar-capillary membrane and subsequent inflammatory infiltration and is associated with high mortality rates, suggesting that new therapeutic strategies are urgently needed.

The recent Concentrated IgM for Application (CIGMA) trial demonstrated that administration of Trimodulin (an IgM/IgA-enriched polyvalent antibody preparation) significantly improved survival in a subgroup of patients with severe community-acquired pneumonia who were being mechanically ventilated, those with the highest inflammatory markers. Immunomodulators have long been considered as potential adjuvant therapies in the treatment of pneumonia but have a mixed record in the literature. In the case of Trimodulin to which extent the benefit is gleaned from its anti-bacterial or anti-inflammatory effects, with respect to pneumonia, or its ability to limit ventilator-induced lung injury is unclear.

We set out to determine the efficacy of Trimodulin and its effect on inflammation and lung barrier permeability in ventilator-induced lung injury by utilizing a well-established murine model. We exposed the mouse subjects to either non-ventilation or high-tidal volume ventilation and treated them with either a control placebo or Trimodulin. Ventilator parameters were taken, and blood and tissue samples were extracted to establish the haematological, biochemical and immunological differences between the groups. Samples were also taken for histopathological examination.

We observed a significant reduction in ventilator pressures and elastance and increased compliance in high-tidal volume ventilated mice treated with Trimodulin. Furthermore, the Trimodulin-treated mice exhibited differentially reduced neutrophil infiltration into lung tissue as well as discrete alterations in cytokine profile consistent with a possible shift towards an anti-inflammatory environment. We conclude that Trimodulin reduced the impact of mechanical ventilation on the lungs in this model. Further studies are required to fully elucidate the mechanism behind clinical responses observed in patients being mechanically ventilated for severe pneumonia and treated with Trimodulin.

4. Zusammenfassung

In ihrer schwersten Form erfordert die ambulant erworbene Pneumonie (engl. community-acquired pneumonia, CAP) mechanische Beatmung, eine lebensrettende Intervention zur Verhinderung eines akuten Atemversagens. Die mechanische Beatmung ist an sich nicht ohne Risiken; eine allgemein anerkannte gravierende Komplikation ist ein beatmungsinduzierter Lungenschaden. Dieser induzierte Lungenschaden ist gekennzeichnet durch eine Zerstörung der alveolo-kapillären Membran mit anschließender entzündlicher Infiltration und ist assoziiert mit hohen Mortalitätsraten - daher sind neue therapeutische Strategien dringend erforderlich.

Die aktuelle CIGMA (Concentrated IgM for Application)-Studie zeigte, dass eine Behandlung mit Trimodulin - eine mit IgM/IgA-angereicherte Präparation eines polyvalenten Antikörpers - die Überlebensrate bei mechanisch beatmeten Patienten mit schwerer ambulant erworbener Pneumonie und erhöhten Entzündungsmarkern signifikant verbessert. Immunmodulatoren werden seit langem als potenzielle Adjuvant-Therapie bei Pneumonien in Betracht gezogen, werden aber in der Literatur unterschiedlich bewertet. Im Fall Trimodulin ist nicht geklärt, welcher Anteil des therapeutischen Nutzens antibakteriellen oder anti-inflammatorischen Effekten bei einer Pneumonie bzw. der Begrenzung des beatmungsinduzierten Lungenschadens zuzuschreiben ist.

Ziel der vorliegenden Arbeit war eine Untersuchung der Wirksamkeit von Trimodulin und seiner Effekte auf Entzündung und Permeabilität der Lungenbarriere beim beatmungsinduzierten Lungenschaden in einem gut etablierten Mausmodell. Wir beatmeten Mäuse entweder nicht oder mit hohem Atemzugvolumen und behandelten sie mit Placebo oder Trimodulin. Beatmungsparameter wurden gemessen und Blut- und Gewebeproben entnommen, um die hämatologischen, biochemischen und immunologischen Unterschiede zwischen den verschiedenen Gruppen zu ermitteln. Darüber hinaus wurden Proben für histopathologische Untersuchungen entnommen.

Wir beobachteten eine signifikante Reduktion von Beatmungsdruck und Elastizität sowie eine erhöhte Lungencompliance bei den mit Trimodulin behandelten und mit hohem Atemzugvolumen beatmeten Mäusen. Zusätzlich zeigten die mit Trimodulin behandelten Mäuse eine differenziell reduzierte Infiltration von Neutrophilen in das Lungengewebe sowie diskrete Veränderungen des Zytokinprofils - vereinbar mit der Annahme einer Verschiebung zugunsten eines mehr entzündungshemmenden

Umfelds. Wir folgern, dass Trimodulin in diesem Modell beatmungsinduzierte Lungenschäden reduzierte. Zusätzliche Untersuchungen sind erforderlich, um den Mechanismus der klinischen Reaktionen bei mechanisch beatmeten und mit Trimodulin behandelten Patienten mit schwerer Pneumonie voll aufzuklären.

5. Introduction

5.1. Community-Acquired Pneumonia

5.1.1. Disease Burden

Community-acquired pneumonia (CAP) refers to the pathological condition of acute pulmonary parenchymal infection acquired outside of hospital settings. It presents a significant health challenge globally, with high rates of morbidity and mortality. In Germany, pneumonia was ranked eighth amongst the most frequent causes of mortality in 2015, with 19,368 deaths attributed to its cause (1). Of those patients diagnosed with CAP, 46.5% require hospitalization (2), generating a significant demand on health services. Furthermore, the toll remains heavy despite improvements in antibiotics and high dependency care, with mortality rates for CAP in Germany standing at 12-13% (3) but increasing with patient's age (4) and infection severity (5).

5.1.2. Immune Response

During pneumonia infection, adhesion of the microbe to the pulmonary epithelia as well as contact with resident immune cells, most likely macrophages, triggers the innate immune response (6). Evolutionarily-conserved bacterial motifs called pathogen-associated molecular patterns (PAMPs) are recognised by pathogen recognition receptors (PRRs) located on immune and epithelial cells (7). Similarly, endogenous molecules released by aggravated tissue called danger-associated molecular patterns (DAMPs) also trigger the PRR system (8). The downstream transcriptional consequence of their activation is the upregulation of nuclear factor kappa-light-chain-enhancer of activated B cells (NF-κB) and interferon regulatory factors 3 and 7 (IRF-3/7). They drive the inflammatory response through production of cytokines (e.g. interleukin (IL)-1β, IL-6, interferon (IFN)-α, IFN-β, tumour necrosis factor (TNF)-α and chemokines (e.g. CXC motif ligand (CXCL)1, CXCL5 and chemokine ligand (CCL)2). These molecules are crucial to innate immunity by activating the acute phase response and recruiting neutrophils and monocytes (9). This pathway is shown in Figure 1.

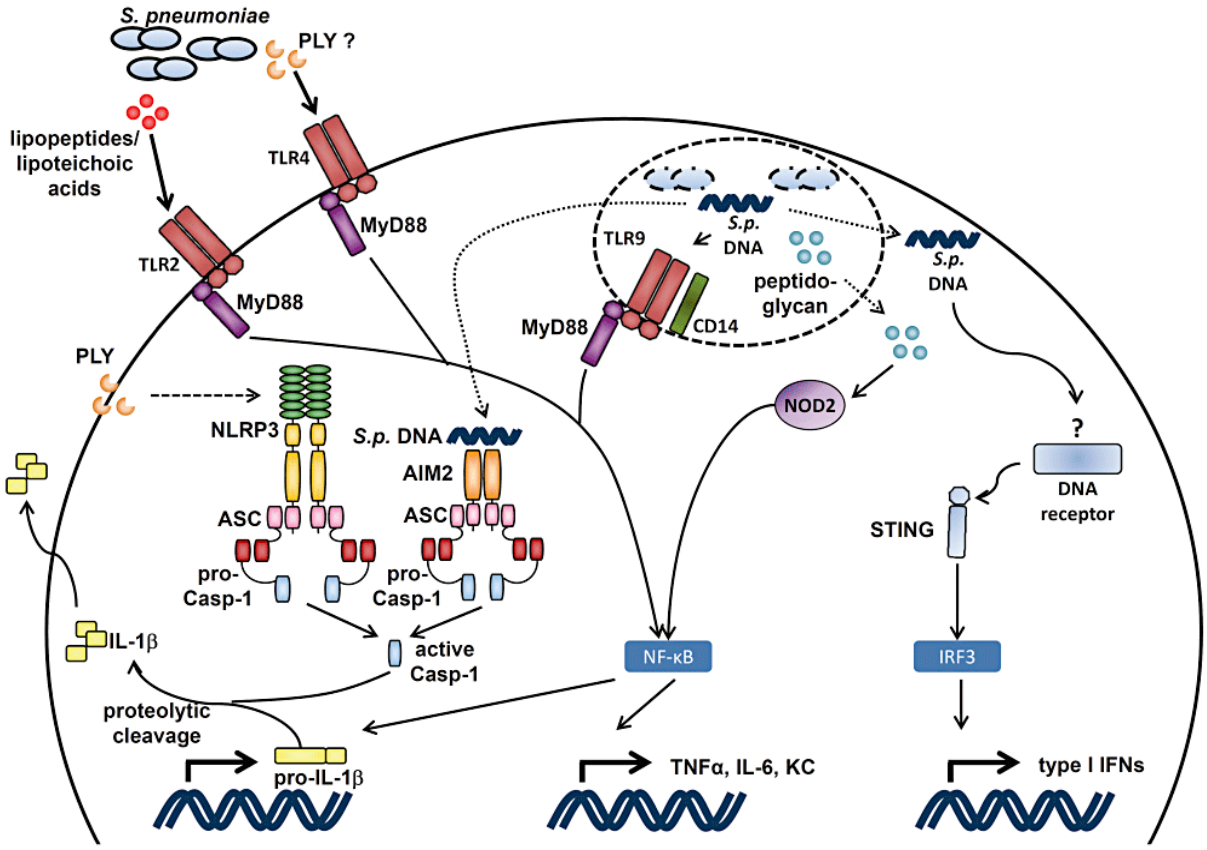

Figure 1. Schematic diagram of pathogen-associated molecular patterns (PAMPs) interaction with Toll-like receptors (TLRs) and downstream transcriptional events triggered by activation. PLY = pneumolysin. Modified from Figure 1 of Koppe et al. 2012 (6). Reproduced with kind permission of John Wiley and Sons.

The main effector cells of the innate immune response to pneumococcal infection are polymorphonuclear cells (PMNs), or neutrophils. They demonstrate effective bacterial killing functions through production of reactive oxygen species (ROS) (10), release of azurophilic granules with lysozymal activity (11), release of neutrophil extracellular traps (NETs) (12) and phagocytosis. Another important player are monocytes, which normally reside in the circulation and are recruited to the site of infection in a CCL2-chemokine receptor (CCR)2 -dependent manner (13). Recruitment and ligation of their PRRs with PAMPs promotes monocytes to differentiate into inflammatory macrophages. After subsequent infiltration of the lung tissue they deploy their effector functions through phagocytosis of bacteria and production of myeloperoxidase (MPO) and superoxide, as well as release of pro-inflammatory cytokines (14).

5.1.3. Current treatment options for CAP

Current recommendations by the Infectious Disease Society of America (IDSA), American Thoracic Society (ATS) (15) and British Thoracic Society (BTS) (16) advise a combination of beta-lactam, macrolide or fluoroquinolone antibiotics for treatment of CAP dependent on the severity of the infection and the status of the patient. There is an emphasis on expedient antibiotic prescription, as studies show a deterioration in survival with administration of antibiotics over four hours after presentation (17).

Severe community-acquired pneumonia (sCAP) is characterized by infiltration of pathogens into the circulatory system. This provokes a systemic response that may become dysregulated and lead to multi-organ dysfunction. Consequently, sCAP is universally accepted to require high dependency supportive care in intensive care units (ICU) because of the need for mechanical ventilation (18) for treatment of respiratory failure.

5.2. Ventilator-induced lung injury

5.2.1. Mechanical Ventilation

Mechanical ventilation (MV) is a life-saving intervention in the context of acute respiratory failure in CAP, defined by acute onset of insufficient oxygenation or insufficient alveolar ventilation or both (19). MV can partially or fully replace spontaneous breathing by facilitating alveolar gaseous exchange and relieving the burden on the respiratory muscles, thereby allowing recovery of their function. It functions via a positive pressure system to drive air into the airways and inflate the alveoli. Consequently, intra-alveolar pressure increases are detected by the ventilator and a termination signal is triggered to stop forcing air into the airways. This termination signal can either be a result of the pre-determined volume of air having been delivered (volume control) or the pre-determined intra-alveolar pressure having been reached (pressure control). There are also various levels of support settings to facilitate greater or less spontaneous effort from the patient. Once the termination signal is executed, central airway pressure falls, and expiration is facilitated passively (20).

5.2.2. Definition of ventilator-induced lung injury

Prolonged exposure of the lungs to the high tidal volumes of MV can provoke the undesired complication of ventilator-induced lung injury (VILI). The phenomena was first noted in 1967 after post-mortems of ventilated patients exhibited significant damage to hyaline membranes with diffuses alveolar infiltrates (21). Patients typically present with worsening hypoxaemia or demand increasing fractions of inspired oxygen (FiO_2). Radiologically there is evidence of bilateral interstitial or alveolar, heterogenous consolidation and atelectasis. The disorder is almost indistinguishable from adult respiratory distress syndrome (ARDS) although its aetiology is entirely iatrogenic in nature. Irrespective, the ramifications of VILI are devastating, with one study demonstrating a mortality of 30-46% in acute lung injury (22).

5.2.3. Mechanism of VILI

The pathological mechanism of lung injury in VILI involves two principal models.

The first model has been historically referred to as *barotrauma.* Sufficient mechanical stress to cause VILI can occur at both high (absolute) lung volumes and relatively low tidal volumes (23). Animal models have shown that this is more reflective of increased lung stretching and higher tidal volumes rather than higher airway pressures (24). The alveolus, the main gas-exchange unit of the lungs, is a sac comprising a fragile layer of epithelial cells (Type I cells) surrounded by capillary blood vessels. Consequently, over-distension of the alveoli results in their rupture and air leaks, whilst deterioration of the hyaline membrane increases vascular permeability. As such, the term *volutrauma* is now recognized as a more appropriate name for this mechanism.

Additional damage can occur due to repetitive opening of alveolar units (25) and asynchronous recruitment of parts of the lungs. The actual mechanism of damage is thought to result from increased pressure at the air-liquid surface interface (26) and is termed *atelectrauma*.

The second principal model is a biological model of VILI (*biotrauma*), caused by inflammatory aggravation in the alveolar units (27). As a result of direct injury to epithelial lung cells in MV, or the physical force being transduced to activate cell-signaling pathways (mechanotransduction), lung epithelial cells release both

chemotactic and inflammatory mediators (28). Subsequently there is recruitment of inflammatory cells into the alveolar space, which release further cytotoxic inflammatory mediators such as TNF-α and IL-6, damage the alveolar capillary membrane and increase vascular permeability (29). Furthermore, translocation of these inflammatory mediators into the systemic circulation culminates in multi-organ dysfunction, due to Fas ligand-associated apoptosis (30). This process is outlined below in (Figure 2) (31).

In both models there is compromise of the alveolar-capillary membrane with surfactant dysfunction, increase in physiological dead space and resultant disruption of pulmonary gas exchange. This congestion of the alveoli limits its ability to stretch to a given pressure and translates to an impairment in compliance. Increased stiffness of the lung requires ever increasing pressures to ventilate and so a vicious cycle ensues.

The picture is further complicated because the pre-injured lung, is at increased susceptibility to VILI (32). Whilst, VILI also provides fertile ground for the development of sepsis (33), thus unpicking the precise mechanism of action is fraught with difficulty.

Consequently, the exact pathogenesis of VILI has not been elucidated and the current assumption, is that it might involve both *volutrauma* and *biotrauma*.

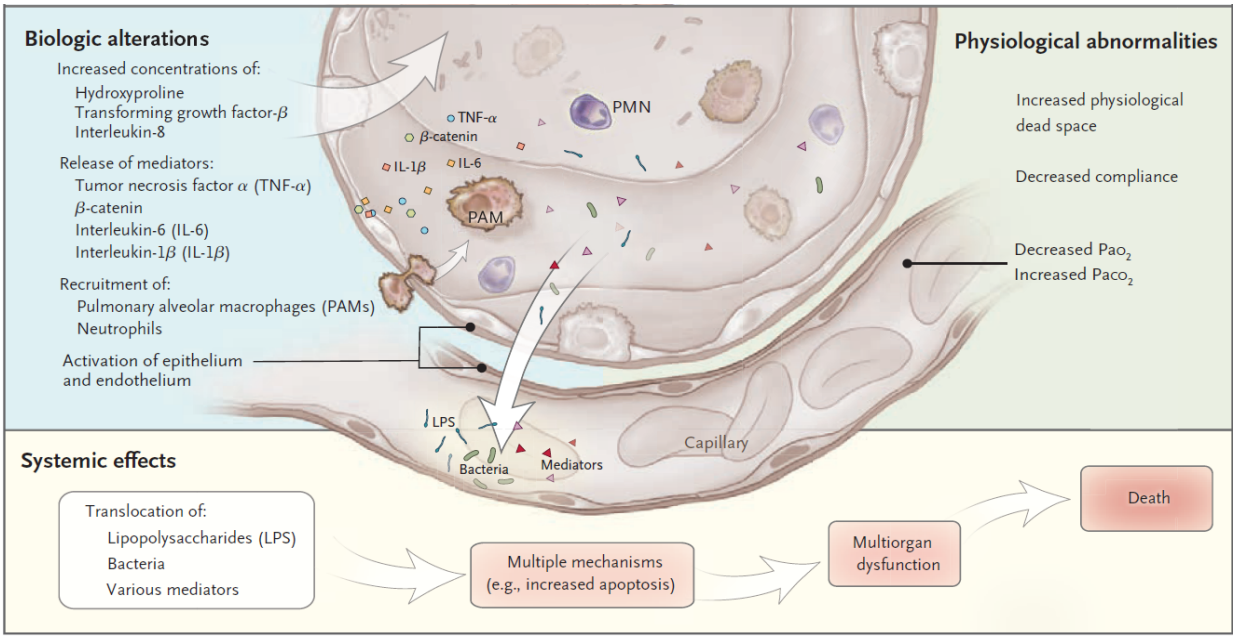

Figure 2. Schematic diagram of alveoli showing both epithelial layer of the alveoli and endothelial layer of the surrounding blood vessels. The biotrauma pathogenic mechanism of ventilator-induced lung injury (VILI) with the subsequent systemic manifestations is exhibited. Modified from Figure 2C of Slutsky et al. 2013 (31). Reproduced with permission from Slutsky et al. 2013 (31). Copyright Massachusetts Medical Society.

5.2.4. Immune Response to VILI

The precise role of the immune system in VILI has not been clearly characterized. IL-1β produced by lung epithelial cells is recognised as a critical inflammatory mediator in the pathogenesis of VILI (34). Its production appears to be driven by a two-signal activation of the NACHT, LRR and PYD domains-containing protein 3 (NLRP3) inflammasome, a multimeric complex that facilitates cleavage of caspase-1, which in turn cleaves inactive IL-1β to produce its active form (35).

The first signal comprises priming of the inflammasome, often through PAMPs. Whereas, the second signal, which induces inflammasome assembly, is typically mediated by DAMPs, produced in response to cellular death or immune activation (36). The combined downstream effect of this is activation of the pro-inflammatory transcription factor NF-κB and subsequent increased transcription and translation of inflammasome components, pro-IL-1β and activation of caspase-1 (37).

However, the inflammasome pathway is also regulated by cytoskeleton responses to cellular stress. In the diseased lung, reduced compliance correlates with increased inflammation as observed in animal models of pulmonary fibrosis (38). Translation of these extracellular stressors into intracellular signalling is called mechanotransduction and has been shown to occur via NLRP3 system in response to the mechanical stress of ventilation (39). This mechanotransduction mechanism is mediated by G-protein signalling secondary to deformation of structural elements of the cell surface. This has been observed with actin depolymerisation in response to mechanical stretch, whereby the NLRP3 inflammasome (40) is activated.

A schematic for the inflammasome-mediated cellular response is shown in Figure 3.

Additionally, more recently the role of cell adhesion molecules, responsible for tethering the cellular cytoskeleton to the extracellular matrix, has been implicated in the pathogenesis of VILI. Downregulation of SRY related High Mobility Group box group-F family member 11 (Sox11) and its downstream effector focal adhesion kinase (FAK) contributed to greater lung injury in a model of VILI (41).

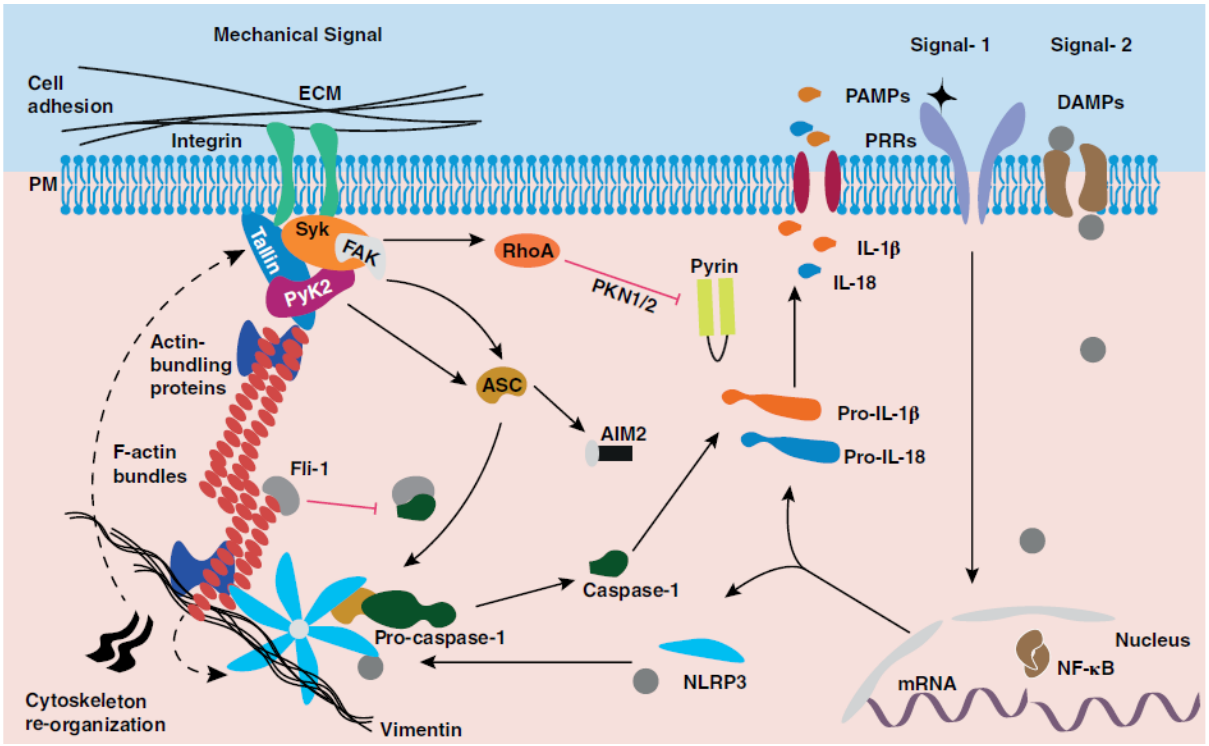

Figure 3. Schematic diagram of cellular inflammasome signalling in response to both mechanical and biological stressors. Mechanotransduction of cellular structural elements regulates activation of the NLRP3 inflammasome. Two-signal activation of PRRs leads to downstream upregulation of the pro-inflammatory transcription factor NF-κB. ECM = extracellular matrix, PM = plasma membrane. Modified from Figure 1 of Joshi et al. 2019 (35). Reproduced with kind permission of John Wiley and Sons.

It is important to note that mechanotransduction of the lung epithelial cells is not solely responsible for the immune response. Similarly, immune cells are also reactive to the mechanical pressures exhibited in VILI. For example, *in vitro* experiments have demonstrated that alveolar macrophages are capable of producing pro-inflammatory cytokines in response to cyclical mechanical stretch (42). Alveolar macrophages have also been shown to be a source of IL-1β through the NLPR3 inflammasome as previously described (39). Furthermore, they are also responsible for increased production of neutrophil chemokines such as IL-8 and CXCL1 and associated increases in alveolar membrane permeability (43). This is suggestive of a significant role for alveolar macrophages in the pathogenesis of VILI.

Neutrophils are considered to play a pivotal part in the development of VILI. Recruitment of neutrophils to the alveoli is increased in VILI. A murine model of VILI demonstrated that increased production of chemokine (CXCL2) appears to be the driving force behind their translocation into the alveolar space (44). However, these neutrophils are not activated until after migration, which appears to be mediated by

their interaction with upregulated CXCR2 ligands (which also included CXCL1 and CXCL3) on the mesenchymal lung tissue in response to mechanical stress (45). The centrality of neutrophils to the pathogenesis of VILI is demonstrated by increased concentrations of neutrophil proteinases in lung injury, which correlates with the severity of the clinicals syndrome (46).

Taken together, there is clearly a strong overlay between the composition of the immunological response to both pneumonia and VILI. We have already noted the increased susceptibility of VILI patients to infection. The immunological aetiology behind this is unknown, but it has been proposed that alveolar over-inflation may increase translocation of bacteria (47) or that the inflammatory milieu generated in response to VILI may inadvertently promote differential bacterial growth (48).

Evidently, the respective immunopathological mechanisms of pneumonia and VILI are difficult to unpick when they occur concurrently. But equally, this presents an opportunity to target both as a potential treatment strategy.

5.2.5. Current treatment options for VILI

Current treatments for VILI rely on application of lung-protective ventilation strategies, such as using low tidal volumes (6 ml/kg instead of 10-15 ml/kg) accompanied by a positive end-expiratory pressure (PEEP). This prevents alveolar collapse at end expiration and improves gaseous exchange (49). One study showed that application of these measures alone reduced the mortality of patients with acute lung injury by 22% (50). However, these strategies run the risk of tipping the balance towards rising partial pressures of carbon dioxide ($PaCO_2$) and respiratory acidosis.

5.3. Prospective therapies

5.3.1. Immunomodulators

As mortality in sCAP and VILI remains stubbornly high, in recent years interest in treatments aimed at addressing the inflammatory-related stress of VILI has increased. So far however, such adjuvant therapies have failed to become clinically established. In the case of the KARE trial, keratinocyte growth factor (KGF) was shown to have no clinical benefit (51). Furthermore, whilst Bellingan et al. (52) have shown impressive

results with the use of interferon-beta-1a (FP-1201) to reduce mortality in ARDS, serious reservations have been raised due to the therapy's potential to induce pulmonary hypertension as an unwanted side effect (53).

Agents designed to modulate the immune system activation have also been proposed as adjuvant therapies. The rationale for this approach was exemplified in one study showing that an increased cytokine response is linked to an increase in mortality in patients with CAP, irrespective of the presence of sepsis (54). Furthermore, a study of ARDS has shown that patients treated in ICU and characterised by higher plasma levels of inflammatory biomarkers have a higher mortality rate and reduced ventilator-free days (55). Whereas, reduced lavage and serum cytokine levels in ventilated VILI patients correlated to a mortality benefit (10).

One such example are statins. They are 3-hydroxy-3-methyl-glutaryl-coenzyme A (HMG CoA) reductase inhibitors, primarily designed to reduce lipid concentrations in patients suffering from hyperlipidaemia and prevent cardiovascular disease. However, they have also been shown to exhibit both anti-inflammatory and anti-microbial effects (56). This laboratory has demonstrated that simvastatin reduces inflammatory markers in a murine model of VILI (57). Unfortunately, these impressive results have not been easily translated into clinical trials. Whilst Makris et al. (58) demonstrated significant improvement in clinical outcomes of patients treated with statins in ventilator-associated pneumonia (VAP), Papazian et al. (59) observed no significant difference in patient outcomes in a similar cohort of patients treated with another statin for VAP.

Collectively, these studies highlight the difficulties of establishing effective adjuvant anti-inflammatory therapies in the treatment of CAP and VILI. However, given the mechanistic crossover of VILI and sCAP, and the significance of inflammation for the pathogenesis of VILI, there is clearly scope for further optimization of the use of anti-inflammatory agents as an adjuvant therapy to traditional antibiotics and lung-protective ventilation. Consequently, other anti-inflammatory targets have come into focus.

5.3.2. Immunoglobulins

One potential therapeutic target identified are immunoglobulins (Ig). The role of immunoglobulin G (IgG) as a component of the adaptive immune response is already well-characterised given their capacity to opsonise pathogens and neutralise endotoxins, e.g. by binding lipopolysaccharide (LPS) (60). However other classes of immunoglobulin are relevant to antibody-mediated immunity.

Immunoglobulin M (IgM) straddles the innate and adaptive immune systems and is an important player in recognising pathogens even without prior immunization by trafficking between the blood and lymph. The pentameric immunoglobulin response functions by opsonising pathogens and directing phagocytosis. The latter alongside its role in interacting with B-cell populations show the immunomodulatory capacity of IgM too (61). In response to tissue injury, DAMPs exposed on the cell surface are recognized by IgM, which subsequently activate complement (62).

Immunoglobulin A (IgA) is the most prominent Ig present at mucosal surfaces, such as the gastrointestinal and respiratory tracts. Although IgA has limited opsonization capabilities and weakly activates the complement system, it binds strongly to the FcαR receptor, expressed on local immune or resident tissue cells (63). This elicits a wide range of biological responses that neutralize invading pathogens.

The rationale for the use of immunoglobulins has been justified by their recognised biological role in pathogen clearance. Neutrophils have been determined to have multiple Fcγ receptors available for binding IgG. The ensuing activation of neutrophils results in upregulation of expression of receptors required for chemoattraction, adhesion and phagocytosis of microbes (64). Conversely in hypogammaglobulinaemic patients with severe sepsis, prognosis is worse with longer duration of shock and more significant lung injury endured (65).

Intravenous immunoglobulin (IVIg) is already used in the treatment of a number of autoimmune conditions. One such example is Kawasaki Disease, whereby there is an inflammatory response to the body's own blood vessels. The NF-κB immune complex is vital in down-stream signalling of IL-1 upregulation in this disease (66), resulting in inflammatory mediator production. IVIg is the main treatment standard for this disease

and has been shown to induce reduced IL-1 activation in peripheral leucocytes and increased induction of IL-1 receptor antagonist (IL-1ra) (67). Similarly, IVIg has an important role in inhibition of downstream effectors as autoantibodies have been identified against a number of cytokines, including TNF-α and IL-2 (68). Cytokine neutralisation is in fact a significant element of the functionality of IVIg.

Meta-analysis by Kreyman et al. (69) of randomized control studies of polyclonal immunoglobulin adjunctive therapies for sepsis demonstrated a significant mortality benefit. Furthermore, this study suggested modest but beneficial outcomes by using polyclonal IgGAM compared to IgG alone. In contrast, more recent meta-analysis by the Cochrane Library (70) revealed that whilst there may be a modest reduction in mortality upon the use of polyclonal immunoglobulin adjunctive therapies, this was not apparent in the highest quality studies with the lowest bias risk. Even more recent data from Vonarburg et al. (71) advocates the use of IgGAM in reducing the occurrence of respiratory infections.

High-quality individual trials have also proven inconclusive to the question of the use of intravenous immunoglobulin (IVIg) in the treatment of ventilator dependent sepsis patients. The SBITS study (72) looked at sepsis patients on ICUs at a number of centres, who were treated with either IVIg or placebo. With respect to their primary endpoint, they noted no significant difference between the groups comparing 28-day mortality. However, the data did demonstrate a significant difference in favour of IVIg in reducing time of mechanical ventilation by 3.0 days (mean 15.0 +/- standard deviation (SD) 10.7 vs. mean 12.0 +/- SD 9.9, $p = 0.009$).

Clearly, more data is required to support the use of IVIG therapy as an adjunctive therapy in the treatment of sepsis. However recent developments in this field have helped to re-ignite the prospects of immunoglobulin therapy.

5.3.3. Trimodulin

The Concentrated IgM for Application (CIGMA) study (73) is the first of its kind to demonstrate positive findings using IgM/IgA-enriched polyvalent antibody preparations in the treatment of mechanically ventilated sCAP patients. Trimodulin is a novel human plasma-derived native polyvalent antibody preparation (contains approximately 23% IgM, 21% IgA and 56% IgG) for intravenous administration which is in development. The company, Biotest AG, has already had success with Pentaglobin, another formulation of IgM-enriched immunoglobulins (12% IgM, 12% IgA and 76% IgG), already approved as adjuvant therapy of severe bacterial infections additional to antibiotic therapy (74).

The phase 2 CIGMA trial was a double-blind randomized study of the effectiveness of Trimodulin as an adjuvant therapy in 160 patients diagnosed with sCAP and requiring mechanical ventilation. Study groups were divided between administration of a control placebo and Trimodulin. Overall, no significant difference in mortality or ventilation-free days was shown between the study groups. However, when post-hoc analysis (to exclude those patients with elements of left ventricular failure) was applied to a selected group of patients with the most significant inflammatory markers (high C-reactive protein (CRP) and/or low basal IgM levels), Trimodulin was shown to significantly reduce absolute mortality and increase the number of ventilator-free days.

The precise mechanism of action of Trimodulin has not been fully characterised. Shankar-Hari et al. (75) undertook a literature review to assess the plausibility of the use of immunoglobulin therapy to treat sepsis in the critical care context. They concluded there are a number of potential mechanisms of action of immunoglobulin therapy: increased bacterial clearance, inhibition of upstream immunological mediators (e.g. NF-κB), increased scavenging of downstream mediators (e.g. cytokines), subversion of inflammation directly through Fc-mediated receptor effects and inhibition of lymphocyte apoptosis, thereby ameliorating septic immunosuppression.

Clearly, further evidence is required to support both the efficacy but also the underlying mechanism of action of polyvalent immunoglobulin preparations in the treatment of patients with sCAP undergoing mechanical ventilation. The question of whether Trimodulin will be an effective adjuvant therapy in this specific subset of these patients (those with significantly raised inflammatory markers) is to be further examined in a phase 3 trial.

6. Project Aims

In the Concentrated IgM for Application (CIGMA) trial Trimodulin, an IgM/IgA-enriched immunoglobulin preparation, was shown to improve the survival of a subset of patients with the most severe form of community-acquired pneumonia, those who require mechanical ventilation with raised inflammatory markers. As these patients suffer from simultaneous impacts of both bacterial infection and ventilation-induced lung injury, it remains unclear what the separate contributions of anti-bacterial, immunomodulatory, and anti-inflammatory effects are to the overall Trimodulin-induced clinical benefit.

These possibilities can be reliably addressed only in a disease model where the effects of Trimodulin on lung injury from infection and from mechanical ventilation are individually assessed. Therefore, we sought to determine the effect of Trimodulin in a murine model of ventilation-induced lung injury in the absence of bacterial infection (sterile inflammation). We aimed to elucidate the impact of the drug on vital and ventilation parameters, cellular migration patterns, and inflammatory cytokine levels. These studies could have translational implications in determining in which patients this adjuvant therapy would be most beneficial.

7. Materials and Methods

7.1. Materials

7.1.1. Instruments

Table 1. Instruments used during the course of the experiments

Instrument	Specification	Company
Animal Restrainer		Charité Berlin (Germany)
Autoclave	Tuttnauer Systec 2540 EL	Systec (Germany)
Blood gas analyzer	ABL 800 Flex	Radiometer (Denmark)
Centrifuge	Megafuge® 1.0R	Heraeus Holding (Germany)
Centrifuge	Biofuge® fresco	Heraeus Holding (Germany)
Dissociator	gentleMACS™ Dissociator	Miltenyi Biotec (Germany)
Flow cytometer	BD FACSCanto II	Becton Dickinson (USA)
Heating Pad	Panlab temperature control unit HB 101/2	Harvard Apparatus (USA)
Laminar flow hood	Hera Safe Type HS 12	Kendro Laboratory Products (USA)
Microplate Photometer	Multiskan™ FC	Thermo Fisher Scientific (USA)
Pipettes	Research® plus	Eppendorf AG (Germany)
Red light	Bosotherm 4000	Bosch + Sohn (Germany)
Scales	LS2000H	G&G (Germany)
Surgical instruments		Fine Science Tools (Germany)
Thermometer	BAT-12 Microprobe Thermometer	Physitemp Instruments (USA)
Tracheal cannula		Hugo Sachs Elektronik (Germany)
Ventilator	flexiVent	SCIREQ (Canada)
Vital parameters monitor	Servomed Patient Monitor	Hellige (Germany)

Vortexer	Vortex-Genie 2® Model G-560E	Scientific Industries (USA)

7.1.2. Consumables

Table 2. Consumables used during the course of the experiments

Product	**Specification**	**Company**
18 G Needle	Sterican® G 18 x 1/2”	B. Braun (Germany)
20 G Needle	Sterican® G 20 x 1/2”	B. Braun (Germany)
26 G Needle	Sterican® G 26 x 1/2”	B. Braun (Germany)
27 G Needle	Sterican® G 27 x 1/2”	B. Braun (Germany)
24 G Cannula	BD Neoflon™	Becton Dickinson (USA)
Blood gas syringe (2 ml)	PICO50 aspirator syringe	Radiometer (Denmark)
Cell strainer (70 µm)	EASYstrainer™ cell strainer	Greiner Bio-One (Austria)
Eppendorf tube (0.5, 1.5 ml)	SafeSeal Micro Tubes	Sarstedt (Germany)
ELISA plate	Microtest Plate 96 Well	Sarstedt (Germany)
EDTA collection tube	Microvette® 500 µl, K3 EDTA	Sarstedt (Germany)
Gloves		B. Braun (Germany)
Histology embedding cassette		Carl Roth (Germany)
Petri dish	TC Dish 60 Standard	Sarstedt (Germany)
Pipette tip (20, 1000 µl)	epT.I.P.S.® Standard	Eppendorf AG (Germany)
Pipette tips (200 µl)		Sarstedt (Germany)
Reaction tube for FACS (5 ml)	Falcon® 5 ml round bottom high clarity PP test tube	Corning (USA)
Reaction tube (15, 50 ml)	Falcon® conical centrifuge tube	Corning (USA)
Syringe (1 ml)	Omnifix® F Solo (1 ml)	B. Braun (Germany)
Syringe (2, 5, 10 ml)	BD Discardit™ II	Becton Dickinson (USA)

7.1.3. Reagents

Table 3. Reagents used during the course of the experiments

Reagent	Company
Complete™, Mini Protease Inhibitor Cocktail	Roche Diagnostics (Germany)
CountBright™ Absolute Counting Beads	Thermo Fisher Scientific (USA)
Ethanol, absolute	Merck (Germany)
FACSFlow™	Becton Dickinson (USA)
FACS™ Shutdown Solution	Becton Dickinson (USA)
Isotonic saline solution (NaCl) 0.9 %	B. Braun (Germany)

7.1.4. Enzymes

Table 4. Enzymes used during the course of the experiments

Enzyme	Company
Collagenase II	Biochrom (Germany)
DNAse I	AppliChem (Germany)

7.1.5. Antibodies for flow cytometry

Table 5. Antibodies for flow cytometry used during the course of the experiments

Epitope	Clone	Fluorochrome	Concentration	Company
CD11b	M1/70	PE-Cy7	0.2 mg/ml	Thermo Fisher Scientific (USA)
CD11c	HL3	APC	0.2 mg/ml	Becton Dickinson (USA)
CD16/32	2.4G2	Unconjugated	0.5 mg/ml	Becton Dickinson (USA)
CD45	30-F11	FITC	0.5 mg/ml	Becton Dickinson (USA)
F4/80	BM8	PE	0.2 mg/ml	Thermo Fisher Scientific (USA)
Ly6C	HK1.4	BV510	100 µg/ml	BioLegend (USA)
Ly6G	1A8	PerCP-Cy5.5	0.5 mg/ml	Becton Dickinson (USA)
MHCII	M6/114.15.2	AlexaFluor 700	0.2 mg/ml	Thermo Fisher Scientific (USA)
Siglec F	E50-2440	BV421	0.5 mg/ml	Becton Dickinson (USA)

7.1.6. Buffers and mediums

Table 6. Buffers used during the course of the experiments

Buffer	Constituents	Company
1x PBS	Dulbecco's phosphate-buffered saline (PBS)	Thermo Fisher Scientific (USA)
FACS Buffer	1x PBS 0.2% Bovine Serum Albumin (BSA)	Thermo Fisher Scientific (USA) Sigma-Aldrich Chemie (Germany)
VILI Buffer	9.75 ml Jonosteril® 0.25 ml tromethamine	Fresenius Kabi (Germany) Köhler Pharma (Germany)
Red Cell Lysis Buffer	1000 ml distilled water, pH 7.5 1 g KHCO3 (0.01 M) 8.29 g NH4C (0.155 M)	B. Braun (Germany) Merck (Germany) Thermo Fisher Scientific (USA)

Table 7. Mediums used during the course of the experiments

Medium	Constituents	Company
1% formaldehyde	1 ml 37% formaldehyde, methanol-free 36 ml 1x PBS	Carl Roth (Germany) Thermo Fisher Scientific (USA)
cRPMI-10	Roswell Park Memorial Institute (RPMI) 1640 Medium 1% L-Glutamine (0.2 M, 100x) 1 % Penicillin/Streptomycin (10,000 U/ml) 1% HEPES buffer (1 M) 10% heat inactivated (30 min, 56°C) Fetal Bovine Serum (FBS)	Thermo Fisher Scientific (USA) Thermo Fisher Scientific (USA) Thermo Fisher Scientific (USA) Thermo Fisher Scientific (USA) CAPRICORN Scientific (Germany)
Heparin	1 ml Heparin (5000 U/ml) 1 ml Sodium Chloride (NaCl)	Ratiopharm (Germany) B. Braun (Germany)

7.1.7. Kits

Table 8. Kits used during the course of the experiments

Kit	Company
Mouse Complement C5a DuoSet ELISA kit	R&D Systems (USA)
Mouse Albumin (Mouse) ELISA Kit	Bethyl Laboratories (USA)
LEGENDplex™ Mouse Anti-Virus Response Panel	BioLegend (USA)

7.1.8. Anaesthesia

Table 9. Anaesthetic agents used during the course of the experiments

Narcosis	Constituents	Company
For Ventilation	1 ml Fentanyl (0.5 mg/10 ml)	Panpharma (France)
	1 ml Medetomidine (Cepetor)	CP-Pharma (Germany)
	1 ml 0.9% NaCl	B. Braun (Germany)
	1 ml Midazolam (Dormicum)	Roche (Switzerland)

7.1.9. Software

Table 10. Software used during the course of the experiments

Software	Company
GraphPad Prism, Version 6	GraphPad Software (USA)
FACS Diva	BD (Germany)
SkanIt 4.1	Thermo Fisher Scientific (USA)

7.2. Methods

7.2.1. Mice and study approval

Female C57BL/6J mice (Janvier Laboratories, France) were used, aged between 69-79 days and weighing 17.20-22.80 grams. Mice were housed in a specific pathogen-free environment with access to food and water *ad libitum* and a 12-hour diurnal cycle. Animal housing and experimental procedures were approved and complied with the Federation of European Laboratory Animal Science Associations (FELASA) guidelines and recommendations for the care and use of laboratory animals.

Study approval was provided by Landesamt für Gesundheit und Soziales (LAGeSo) Berlin on 26th March 2019 (Reference Number/Anzeigenummer A 0040/19).

The experimental groups are outlined below:

Table 11. Division of mice into experimental groups

Experimental Group	Number
High Tidal Volume (HVT) + Trimodulin	11
High Tidal Volume (HVT) + control (formulation buffer)	11
Non-ventilated (NV) + Trimodulin	11
Non-ventilated (NV) + control (formulation buffer)	11

7.2.2. Trimodulin treatment

Mice received intravenous tail injections of either 384 mg/kg Trimodulin (Batch B588029; Biotest AG, Germany) or equivalent dose of the Trimodulin formulation buffer as control (Biotest AG, Germany) at 30 minutes prior to initiation of ventilation or non-ventilation.

7.2.3. Mechanical ventilation

Mice were anaesthetized with a 100-120 µl intraperitoneal injection of Fentanyl (0.05 mg/kg), midazolam (*Dormitor*®) (5 mg/kg) and medetomidine (*Cepetor*®) (0.5 mg/kg) (FMM). An intraperitoneal catheter was introduced to provide access for further infiltration of anaesthesia during the procedure. A heating pad and anal measurement probe (Harvard Apparatus, USA) were used to maintain the body temperature at 37°C.

After anaesthesia a tracheotomy was made, and the mouse was intubated with a tracheal cannula. The mice were ventilated with a flexiVent™ mechanical ventilator (SCIREQ, Canada) initially at a low tidal volume (LVT) setting (tidal volume (VT) = 9 ml/kg, respiratory rate (RR) = 160 bpm, positive end-expiratory pressure (PEEP) = 2 cmH_2O, inspiratory: expiratory ratio (I:E) = 50%). A Luminject® catheter (Transcodent, Germany) was introduced into the left common carotid artery to provide central arterial pressure monitoring and pressure support with an infusion of a balanced electrolyte buffer (Jonosteril, Germany) with 0.0075 mmol/ml tromethamine (Köhler Pharma GmbH, Germany) at 350 µl/h. Vital parameters were monitored continuously using a Servomed Patient Monitor (Hellige, Germany). A 24G urinary catheter (Becton Dickinson Infusion, USA) was inserted into the urethra for fluid balance monitoring.

Recruitment manoeuvres were subsequently performed. Mice in the high tidal volume (HVT) group then had their ventilator settings adjusted (VT = 35 ml/kg, RR = 70 bpm, PEEP = 2 cmH_2O, I:E = 50%) and were ventilated for a total of 4 hours. Airway pressure, respiratory rate, and tidal volume were measured at 10-minute intervals for the duration of the experiment. The non-ventilated group underwent all previous steps prior to the HVT ventilation and then were removed from the ventilator.

Ventilation parameters of resistance, compliance and elastance were measured by the flexiWare™ software (SCIREQ, Canada) and extracted at a later date.

All mice survived the protocol. Once the experiments were terminated all mice were euthanized by exsanguination from the common carotid artery catheter.

7.2.4. Blood gas analyses

50 µl heparin (5000 U/ml made up in a 1:1 ratio with 0.9% NaCl) was injected into the carotid artery of the mouse and fresh blood collected into a blood gas syringe containing heparin (PICO50 aspirator syringe, Radiometer, Denmark) to avoid coagulation.

Samples were analyzed immediately using a blood gas analyzer (ABL 800; Radiometer, Denmark) to obtain values for partial pressure of oxygen (PaO_2), partial pressure of carbon dioxide ($PaCO_2$), pH, bicarbonate (HCO_3^-), base excess (SBE), lactate, sodium (Na^+), potassium (K^+), chloride (Cl^-) and calcium (Ca^{2+}).

7.2.5. Blood count

Blood leucocyte and platelet counts were determined immediately using a Scil Vet abc™ Animal Blood Counter (Scil Animal Care Company GmbH, Germany). The remaining blood was centrifuged at 2000 xG for 10 minutes at 4 °C and the plasma extracted and snap frozen. These samples were stored at -80 °C.

7.2.6. Lung leucocyte isolation

In order to reduce the number of blood lymphocytes, the lung tissue was perfused with 10 ml of cooled, sterile 1x PBS (Thermo Fisher Scientific, USA), infused directly into the right ventricle. The left lung was then excised from the thoracic cavity. The lung

was manually cut into small pieces and digested in a collagenase (Biochrom, Germany) and DNAse (AppliChem, Germany) solution for 30 minutes at 37 °C. A single cell suspension of the lung digestion was obtained by mechanical disruption through a 70 µm cell strainer (Greiner Bio-One, Austria). This was washed in cRPMI and centrifuged at 470 xG for 5 minutes at 4 °C to pellet the cell suspension. The pellet was resuspended in FACS buffer and used for flowcytometric analysis as outlined below in 7.2.8.

The residual right lung was suspended in 1 ml of PBS and dissociated using a gentleMACS™ Dissociator (Miltenyi Biotec, Germany) and snap frozen. These samples were stored at -80 °C.

7.2.7. Bronchoalveolar lavage

Bronchoalveolar lavage (BAL) was performed by flushing through the trachea 800 µL 1 x PBS containing protease inhibitor (complete mini; Roche Diagnostics, Germany). Lavage was performed in total two times. The supernatant (fluid) and pellet (cells) were separated by centrifugation at 470 xG for 5 minutes at 4°C. BAL cells were suspended in staining buffer (see section 7.2.8) and stored at 4°C. The supernatant was frozen in liquid nitrogen at -80°C until required for further analysis.

7.2.8. Differential Cell Counting

Isolated BAL and lung cell samples were blocked with anti-CD16/32 (Becton Dickinson, USA) and stained with anti-CD45 (30-F11; Becton Dickinson, USA), anti-CD11c (HL3; Becton Dickinson, USA), anti-CD11b (M1/70; Thermo Fisher Scientific, USA), anti-F4/80 (BM8; Thermo Fisher Scientific, USA), anti-Ly6C (HK1.4; BioLegend, USA) anti-Ly6G (1A8; Becton Dickinson, USA), anti-MHCII (M6/114.15.2; Thermo Fisher Scientific, USA) and anti-SiglecF (E50-2440; Becton Dickinson, USA) monoclonal antibodies.

Determination of total cell numbers was made using CountBright Absolute Counting Beads (Thermo Fisher Scientific, USA).

Flow cytometry was used to quantify leucocytes on the FACSCanto II machine (Becton Dickinson, USA). Differentiation was made according to their forward and side scatter

profiles and expression of the aforementioned antigens. The gating strategy is shown below in Figure 4.

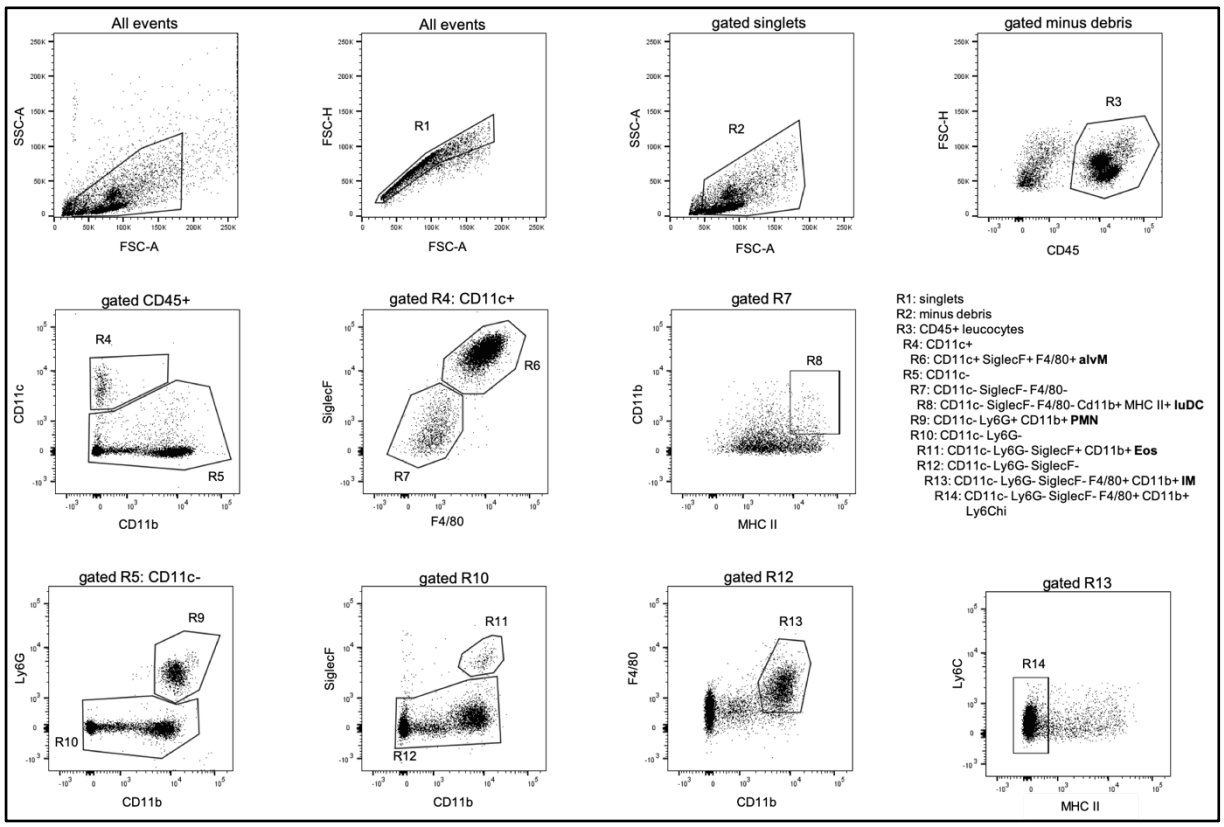

Figure 4. Gating strategy for innate lung leucocytes in FACS analysis

Results were analyzed using BD FACSDiva (Becton Dickinson, USA).

7.2.9. Murine Serum Albumin (MSA) ELISA

Murine alveolar permeability was evaluated using the Mouse Serum Albumin (MSA) enzyme-linked immunosorbent assay (ELISA) Quantitation Set (Bethyl Laboratories, USA). Plasma samples were diluted by between 1:500,000 – 1:750,000 and BALF samples were diluted by 1:1,000 using conjugate diluent. Albumin concentration was quantified according to manufacturer's instructions. The degree of alveolar permeability was determined by the ratio of the BALF and plasma values acquired. This reflects the amount of albumin transferring from the plasma to the alveolar space and is thus an indicator of alveolar permeability.

7.2.10. Inflammatory Cytokine Multiplex ELISA

The LEGENDplex™ Mouse Anti-Virus Response Panel with V-bottomed plate (BioLegend, USA) was used to quantify inflammatory cytokines and chemokines. In total 13 cytokines and chemokines (IFN-γ, CXCL1, TNF-α, CCL2, IL-12, CCL5, IL-1β, CXCL10, GM-CSF, IL-10, IFN-β, IFN-α and IL-6) were measured using the kit. Plasma samples were diluted by 1:1 and BALF samples left undiluted. Concentrations were determined by the forward and side scatter profile measured by flow cytometry (FACS Canto II; Becton Dickinson, USA) according to manufacturer's instructions.

7.2.11. Complement C5a ELISA

Complement C5a concentrations in plasma (diluted 1:10) and BALF (undiluted) were quantified using the Mouse Complement C5a DuoSet ELISA kit (R&D Systems, USA) according to manufacturer's instructions.

7.2.12. Histology

In the case of the histological samples, the mice were sacrificed by exsanguination as described in 7.2.3. The thoracic cavity was opened, and the trachea was exposed. The trachea was then ligated to prevent alveolar collapse. The lungs were carefully excised from the thoracic cavity and fixed in embedding cassettes (Carl Roth, Germany) in 1% formaldehyde methanol-free solution for 24-48 hours at room temperature. The liver, kidney and spleen were also collected in an analogous fashion for histological analysis.

The histological samples were then transported to the pathology laboratory of Univ.-Prof. Dr. Achim Gruber at the Institute of Veterinary Pathology, Freie Universität, Berlin. Here the samples underwent further preparation for histological analysis. The lungs were embedded in paraffin and cut into 2 µm-thick sections. The sections were then stained with haematoxylin and eosin (H&E) as previously described (76). In mechanically ventilated subjects, in addition to the H&E staining, visualization of the connective tissue, basement membrane and cell walls was optimized with a Periodic Acid-Schiff (PAS) stain.

Lung samples were microscopically evaluated for the spread and severity of pathological changes by two independent board-certified veterinary pathologists,

whom were blinded to the study groups. They were given a score of 0-4 for each of six different domains and a total inflammation score (out of 24) generated.

Due to red cast reduction of macro images, color auto-correction using ADOBE® PHOTOSHOP® CS5 Extended, Version 12.0.4 was performed.

The experimental groups are outlined below:

Table 12. Division of mice into experimental groups for histology

Experimental Group	Number
High Tidal Volume (HVT) + Trimodulin	6
High Tidal Volume (HVT) + control (formulation buffer)	6
Non-ventilated (NV) + Trimodulin	6
Non-ventilated (NV) + control (formulation buffer)	6

7.2.13. Statistical Analyses

Measurement data are presented as scatterplots with mean and standard error of the mean (SEM) or as single mean values and SEM. Non-parametric data are presented as scatterplots with median and interquartile range (IQR). For comparison between two groups and grouped analyses, two-way analysis of variance (ANOVA)/ Tukey's multiple comparison test or repeated measures two-way ANOVA was performed. For comparison of non-parametric data, the Mann-Whitney test was performed. *P* values < 0.05 were considered significant. Analyses and graph production were performed using GraphPad Prism, Version 6 (USA).

8. Results

In a reverse translational approach, this project aimed to understand how the protective mechanisms of Trimodulin observed in a subpopulation of patients in the CIGMA trial manifested. This was achieved by utilizing a murine model of VILI to compare two groups of mouse subjects: those injected with a control solution (formulation buffer) and those injected with a pre-established dose of Trimodulin. Both non-ventilated and high-tidal ventilation sub-groups were compared within these groups and parameters were taken on the ventilator. Plasma and BAL samples were also taken to measure the arterial blood gas analyses, haematological and biochemical profiles, cell populations and albumin content. Furthermore, tissue samples were taken in order to analyze whether there was a difference at tissue level between Trimodulin and the control.

8.1. Clinical, Biochemical and Ventilator Parameters with Trimodulin treatment

During the high tidal volume ventilation (HVT), the mice had their clinical parameters monitored every 10 minutes as a measure of their clinical status during the procedure. The parameters measured were mean arterial pressure (MAP), heart rate (HR) and oxygen saturations (SpO_2). Once the experiment ended the mice were euthanized by exsanguination from the common carotid artery catheter. The blood was heparinized, and arterial blood was collected for blood gas analysis. Values were obtained for partial pressure of oxygen (PaO_2), partial pressure of carbon dioxide ($PaCO_2$), pH, bicarbonate (HCO_3^-), base excess (SBE), lactate, sodium (Na^+), potassium (K^+), chloride (Cl^-) and calcium (Ca^{2+}). During the HVT ventilation, the SciREQ flexiVent software automatically records ventilator parameters every 10 minutes. These parameters reflect the health of the lungs during the ventilation. The parameters measured were tracheal pressures, compliance, elastance and resistance.

8.1.1. Clinical status with mechanical ventilation is unaffected by Trimodulin treatment

The mice exhibited a general decrease in their MAP and an increase in their HR during the course of the ventilation. The mice generally maintained their SpO_2 for the first 180 minutes of the ventilation and then demonstrated a decline in the SpO_2 for the last 60

minutes of the procedure. There was no significant difference in MAP, HR or SpO_2 between the control and Trimodulin-treated mice (Figure 5).

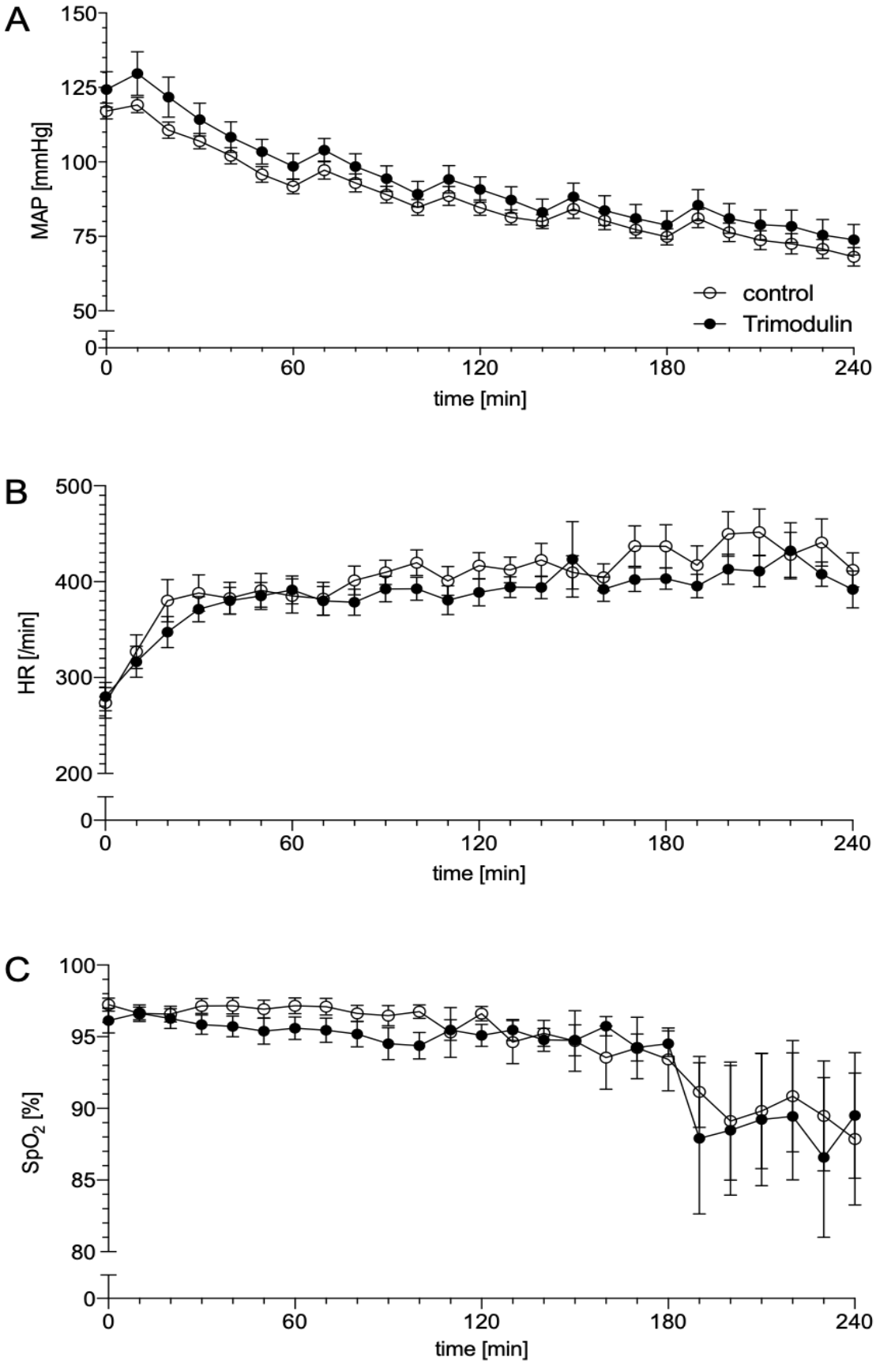

Figure 5. **Clinical parameters were similar between control and Trimodulin-treated mice. A** – mean arterial pressure (MAP), **B** – heart rate (HR), **C** – oxygen saturation (SpO_2) measured at 10-minute intervals during 240 minutes of HVT ventilation. Analyzed using repeated measures two-way ANOVA. Data in A-C display mean, and error bars represent SEM.

8.1.2. Blood gas parameters were stable, independent of Trimodulin treatment

An arterial blood gas analysis provides a snapshot of the current gas exchange capacity of the lung, as well as providing values of electrolytes important to the acid-base balance of the organism.

The pH demonstrated a generalized increase in the HVT group compared to the NV group, but there was no difference between the control and Trimodulin-treated mice in either group (Figure 6A). Similarly, there was a generalized increase in the partial pressure of carbon dioxide ($PaCO_2$) values in the NV group compared to the HVT group and this probably reflects the increased acidity of the arterial blood. However, there was no difference between the control and Trimodulin-treated mice in either group (Figure 6D). The standardized partial pressure of oxygen ($stPaO_2$) was calculated to correlate with its clinical use in establishing accurate alveolar PaO_2. The following formula was used.

$$stPaO_2 = PaO_2 – 1.6 \times (40 – PaCO_2)$$

The results show a generalized decrease in the $stPaO_2$ values in the arterial blood of the HVT group compared to the NV group. However, there was no difference between the control and Trimodulin-treated mice in either group (Figure 6C).

There was no difference observed in the arterial blood bicarbonate (HCO_3^-) values between the HVT or NV groups. Furthermore, there was no difference between the control and Trimodulin-treated mice in either group (Figure 6B).

Base excess (SBE) values in arterial blood were lower in the NV group than the HVT group and likely reflected the decreased pH in this group. But there was no difference between the control and Trimodulin-treated mice in either group (Figure 6E).

Overall, the results demonstrate stable alveolar gas exchange independent of Trimodulin treatment in the two groups.

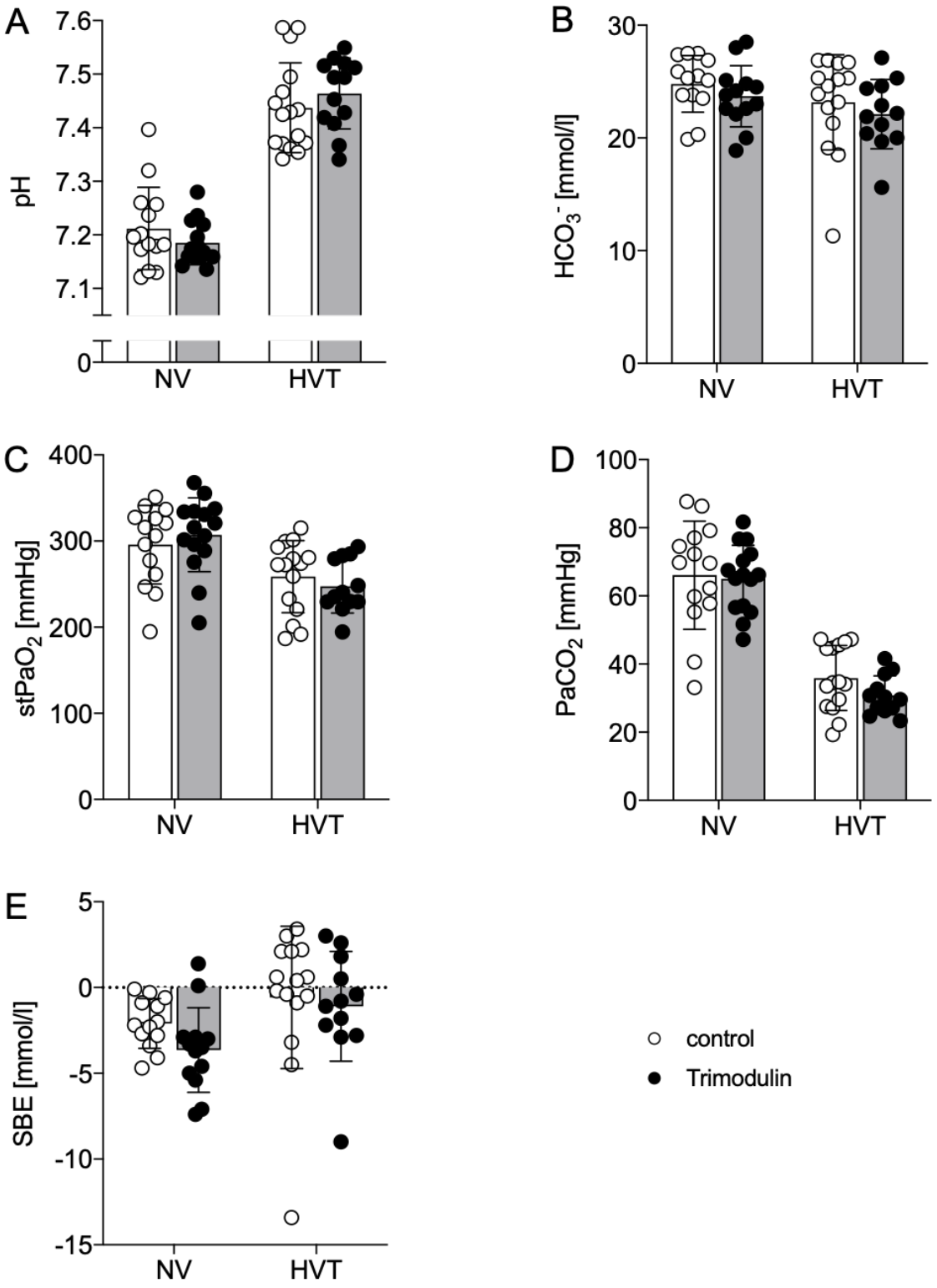

Figure 6. Blood gas parameters were similar between control and Trimodulin-treated mice. A – pH, **B** - bicarbonate (HCO_3^-), **C** – standardized partial pressure of oxygen ($stPaO_2$), **D** - partial pressure of carbon dioxide ($PaCO_2$), **E** – base excess (SBE) in arterial blood after no ventilation (NV) or 4 hours of high tidal volume ventilation (HVT). Analyzed using repeated measures two-way ANOVA/Tukey's multiple comparison test. Data in A-E display mean, and error bars represent SEM.

Arterial blood gas measurements of Sodium (Na^+) showed a significant increase ($P < 0.0001$) in the HVT group compared to the NV group (Figure 7A). This can be explained by a well-renowned renal exchange mechanism whereby H^+ ions are exchanged for Na^+ ions (Na-H antiporter) to maintain acid base balance. This reflects the decreased acidity of the arterial blood in the HVT group (Figure 6A). However, there was no difference between the control and Trimodulin-treated mice in either group. There was no difference between the NV and HVT or control or Trimodulin-treated groups for either Potassium (K^+) (Figure 7B) or Calcium (Ca^{2+}) (Figure 7C) observed in the arterial blood. There was a significant increase ($P < 0.001$) in the concentration of lactate in the HVT group compared to the NV group (Figure 7D). This is in keeping with lung tissue damage and resultant anaerobic respiration. However, there was no difference between the control and Trimodulin-treated mice in either group.

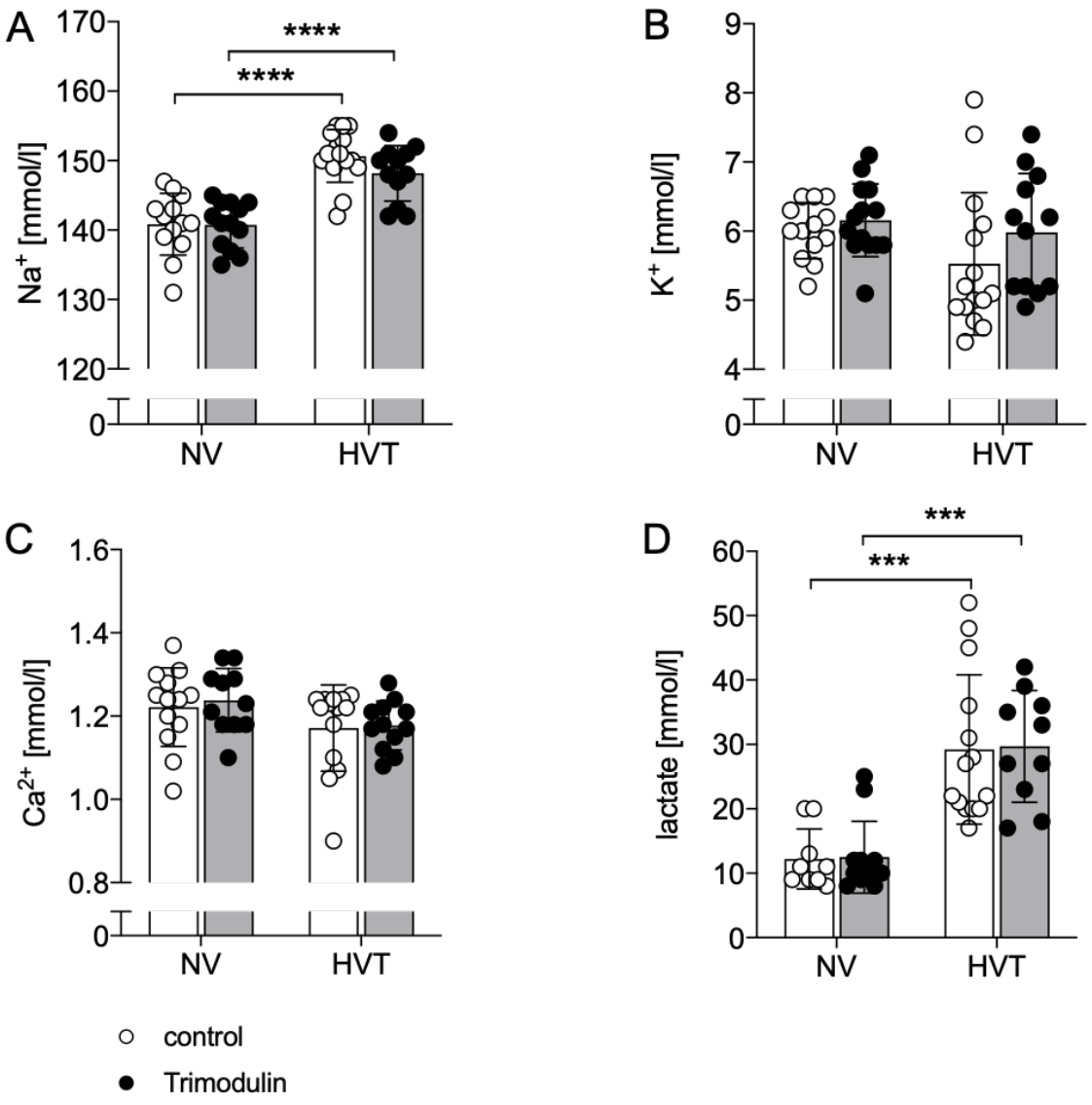

Figure 7. Biochemical parameters were similar between control and Trimodulin-treated mice. A – sodium (Na^+), **B** – potassium (K^+), **C** – calcium (Ca^{2+}), **D** - lactate in arterial blood after no ventilation (NV) or 4 hours of high tidal volume ventilation (HVT). An asterisk (*) denotes statistical difference between NV and HVT groups, analyzed using two-way ANOVA/Tukey's multiple comparisons test. *** denotes P < 0.001. **** denotes P < 0.0001. Data in A-D display mean, and error bars represent SEM.

8.1.3. Increase in airway opening pressure was reduced by Trimodulin treatment

Airway opening pressure (PaO) represents the pressure required to open the alveoli and was measured in the trachea in this model. If the PaO is too great, then damage can be caused to the alveoli through barotrauma.

During HVT ventilation Trimodulin-treated mice demonstrated consistently reduced PaO compared to control mice (Figure 8). This difference across the duration of the ventilation was statistically different (P < 0.0001). This is indicative of reduced transpulmonary pressures reflective of reduced stress on the lung parenchyma.

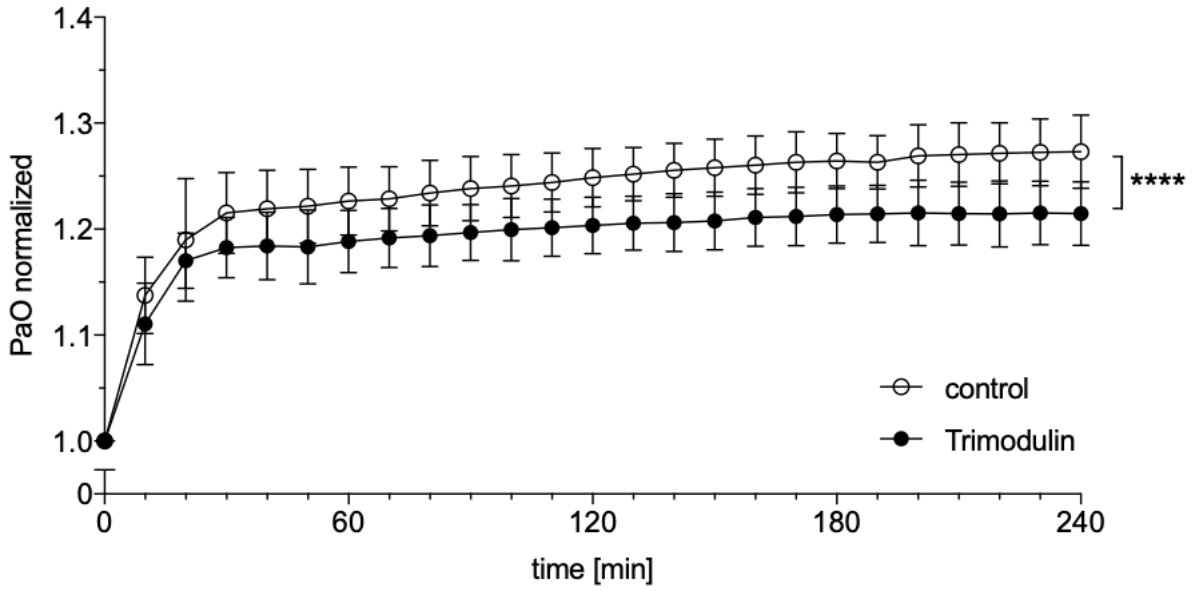

Figure 8. Airway opening pressure is reduced with Trimodulin treatment. Airway opening pressure (PaO) normalized to 1 and measured at 10-minute intervals during 240 minutes of HVT ventilation. An asterisk (*) denotes statistical difference between control and Trimodulin-treated mice, analyzed using repeated measures two-way ANOVA. **** denotes P < 0.0001. Data in figure display mean, and error bars represent SEM.

8.1.4. Lung integrity and function is protected by Trimodulin treatment in HVT

Compliance (C) is the unit measure of the lung's ability to expand, i.e. the elastic forces that limit lung inflation. Compliance is determined by calculating the change of volume of the lungs to a change in pressure. A reduction in compliance is pathological and reflective of a reduced ability of the lung to expand. Elastance (E) is the reciprocal measure of compliance. Therefore, it is the unit measure of the lungs ability to return to its original structure after being distended by external forces. An increase in elastance therefore reflects difficulty in inflating the alveolar units, i.e. the lungs are less compliant. Resistance (R) is a measure of the resistance of the airways to flow of air. In this experiment, this may be provided by the airways of the mouse, the chest wall and resistance provided by the endotracheal tube, which is pathological.

During HVT ventilation the compliance initially falls due to surface tension before levelling out. The reduction in compliance was less in Trimodulin-treated mice compared to control mice (Figure 9) and this difference was statistically different ($P < 0.05$). Increased compliance implies good pliability of the lung and reduced stiffness.

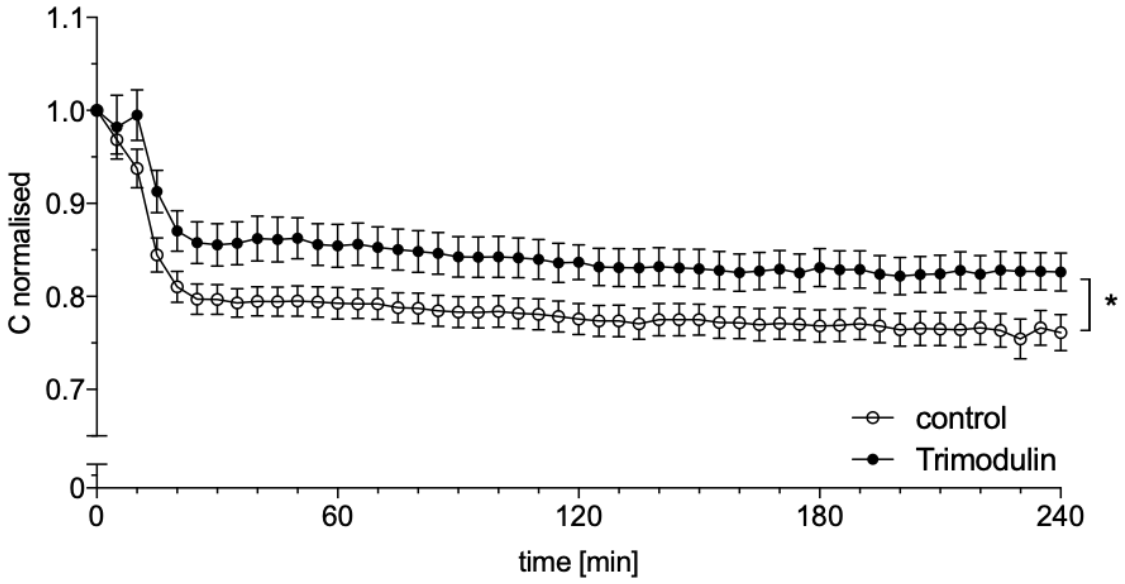

Figure 9. Lung compliance improved with Trimodulin treatment. Compliance (C) normalized to 1 and measured at 5-minute intervals during 240 minutes of HVT ventilation. An asterisk (*) denotes statistical difference between control and Trimodulin-treated mice, analyzed using repeated measures two-way ANOVA. * denotes $P < 0.05$. Data in figure display mean, and error bars represent SEM.

During HVT ventilation both groups saw a reciprocal rise in elastance, but Trimodulin-treated mice demonstrated reduced elastance compared to control mice (Figure 10). This difference was statistically different ($P < 0.05$).

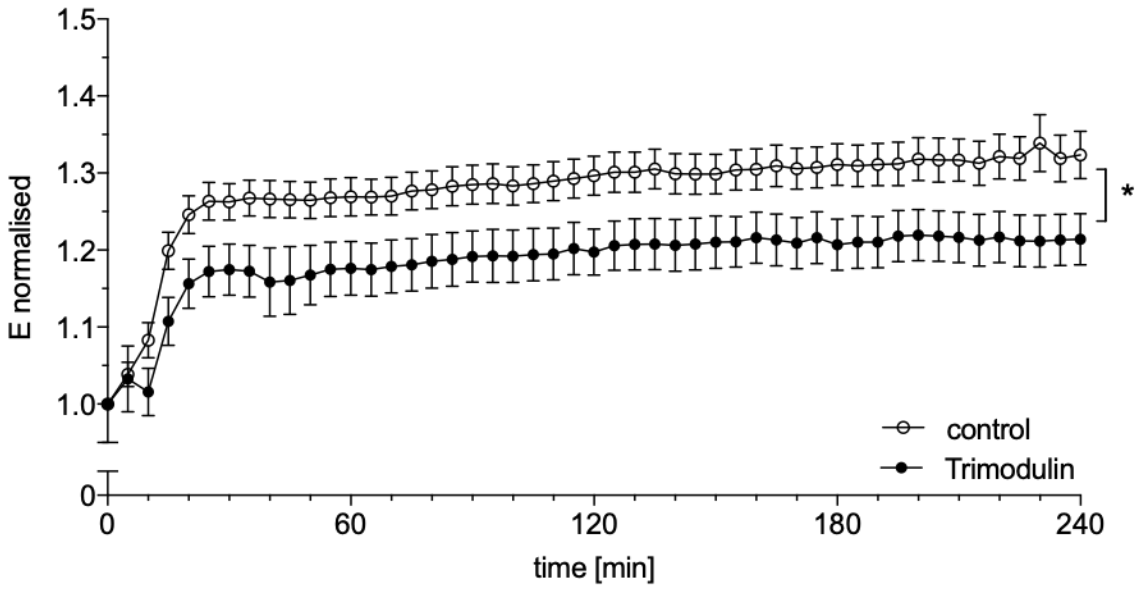

Figure 10. Lung elastance reduced with Trimodulin treatment. Elastance (E) normalized to 1 and measured at 5-minute intervals during 240 minutes of HVT ventilation. An asterisk (*) denotes statistical difference between control and Trimodulin-treated mice, analyzed using repeated measures two-way ANOVA. * denotes $P < 0.05$. Data in figure display mean and error bars represent SEM.

During HVT ventilation there was no statistical difference noted in resistance between control and Trimodulin-treated mice (Figure 11).

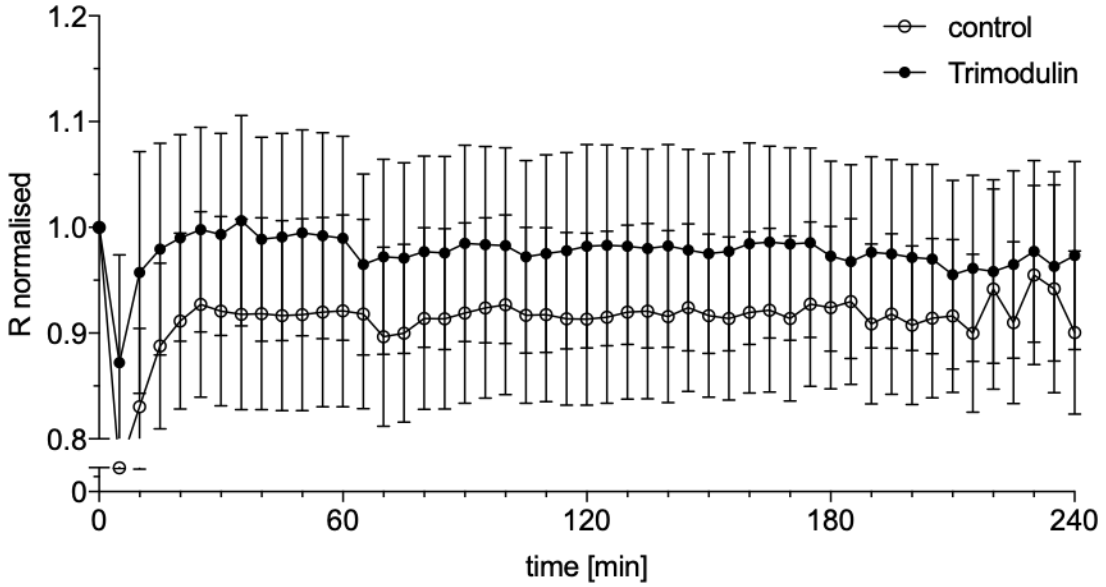

Figure 11. Lung resistance was similar between control and Trimodulin-treated mice. Resistance (R) normalized to 1 and measured at 5-minute intervals during 240 minutes of HVT ventilation. Analyzed using repeated measures two-way ANOVA. Data in figure display mean and error bars represent SEM.

8.2. Lung Permeability and Histopathology

The next part of the study established the degree of lung barrier dysfunction. By measuring the amount of translocated serum albumin from the blood to the alveolar compartment, the degree of lung-vascular permeability could be estimated. Histopathology images demonstrated permeability with microscopic evidence of oedema and hyaline membrane formation. Furthermore, these images were evaluated for histological evidence of cellular infiltration. These combined provided a general inflammation score with which to compare the mice treated with control solution versus Trimodulin-treated mice.

8.2.1. Increase in lung permeability was not prevented by Trimodulin treatment

As expected, there was a significant increase ($P < 0.01$) in mouse lung permeability in the HVT ventilation group compared to the NV ventilation group. There was a moderate trend towards reduced lung permeability between control and Trimodulin-treated mice in the HVT group but this was not statistically significant (Figure 12).

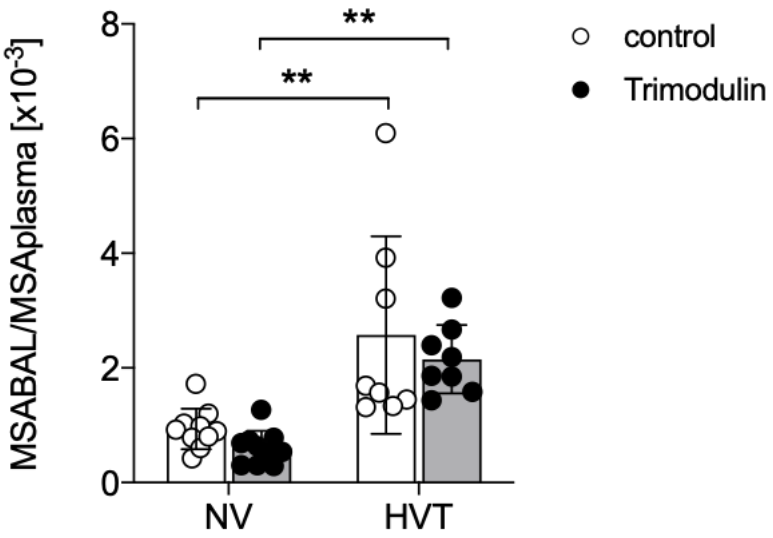

Figure 12. Lung permeability was not improved with Trimodulin treatment. Mouse lung permeability measured as the ratio of mouse albumin concentration in plasma and BAL samples after no ventilation (NV) or 4 hours of high tidal volume ventilation (HVT). An asterisk (*) denotes statistical difference between NV and HVT groups, analyzed using two-way ANOVA/Tukey's multiple comparisons test. ** denotes P < 0.01. Data display mean, and error bars represent SEM.

8.2.2. Lung histopathology was not drastically altered after 4h of ventilation and Trimodulin treatment

Histological quantification of lung injury demonstrated an expected increase in total inflammatory score of lung tissue samples in the HVT group compared to the NV group. There was a general trend towards reduced perivascular oedema and alveolar wall injury in the Trimodulin-treated compared to the control mice in the HVT group (Figure 13). However, these differences were not of statistical significance.

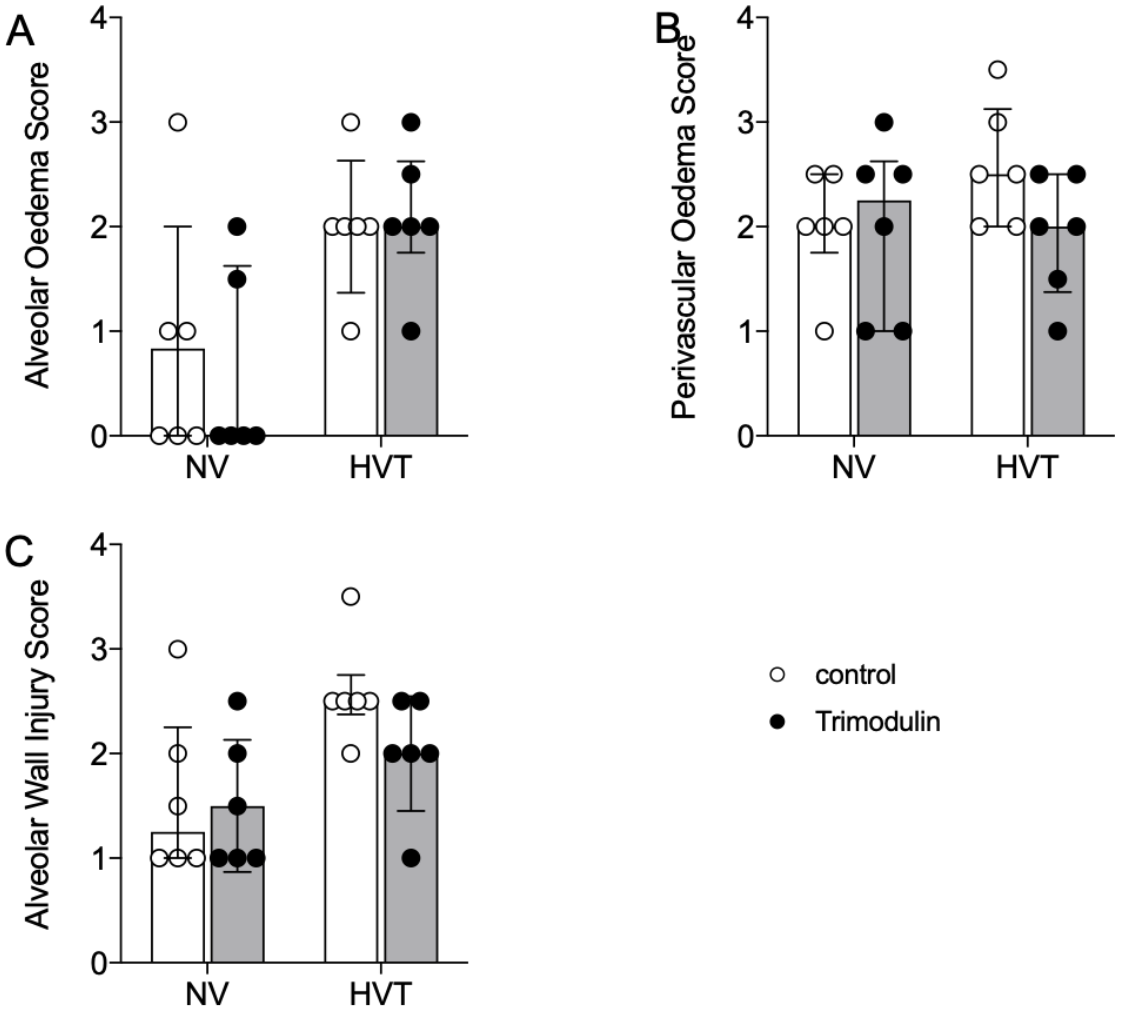

Figure 13. No significant difference in histological alveolar wall injury or oedema scores between control and Trimodulin-treated mice. A – histological alveolar oedema score, **B** - histological perivascular oedema score, **C** - histological alveolar wall injury score of lung tissue after no ventilation (NV) or 4 hours of high tidal volume ventilation (HVT). Analyzed using Mann-Whitney test. Data in A-C display median, and error bars represent IQR.

Similarly, a general reduction in the number of cells in the alveolar space and hyaline membrane was observed in the Trimodulin-treated compared to the control mice in the HVT group (Figure 14). However, these differences were not of statistical significance.

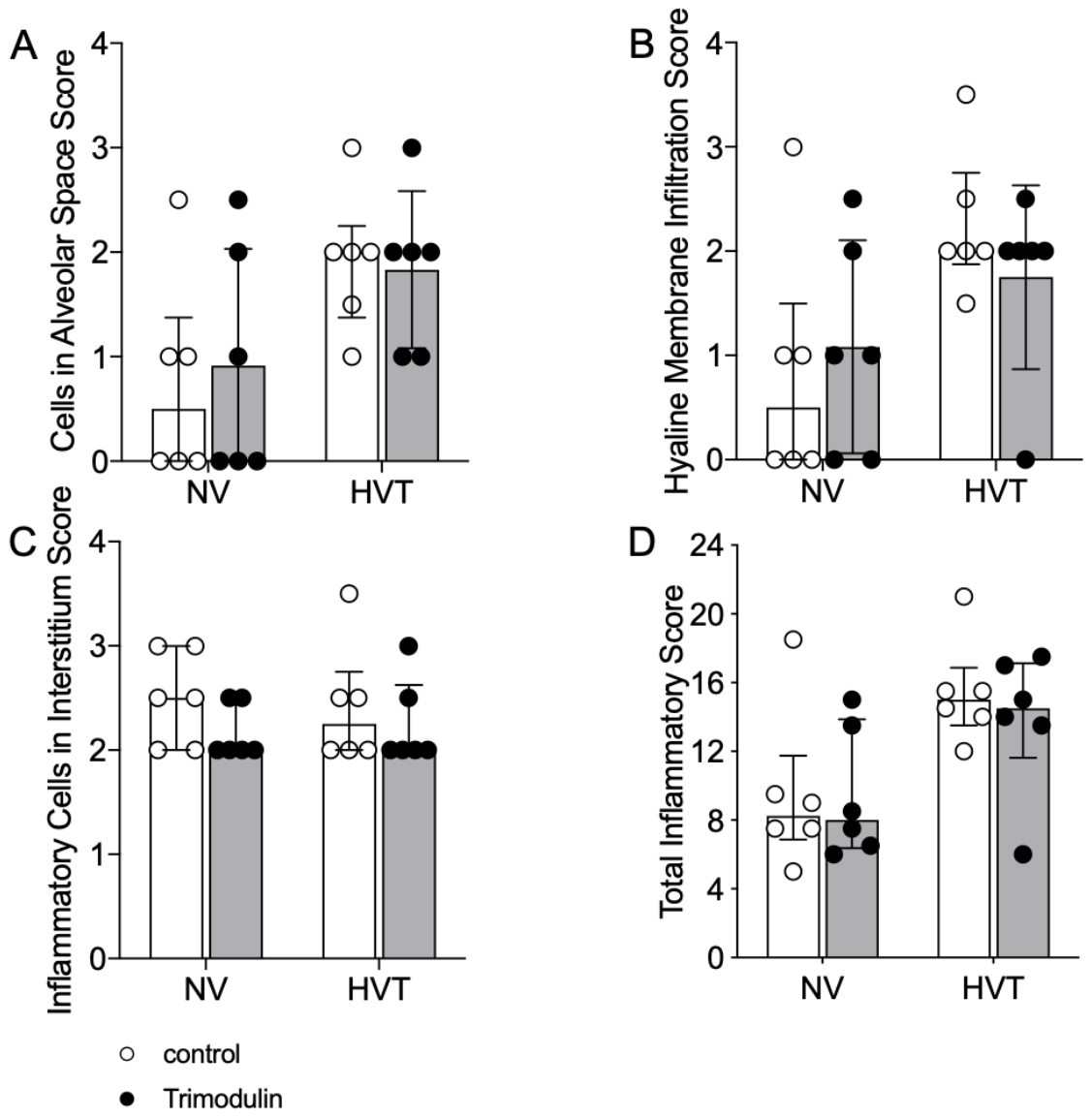

Figure 14. **No significant difference in histological cellularity or total inflammatory scores between control and Trimodulin-treated mice. A** – histological cells in alveolar space score, **B** - histological hyaline membrane infiltration score, **C** - histological inflammatory cells in the interstitium score and **D** – histological total inflammatory score of lung tissue after no ventilation (NV) or 4 hours of high tidal volume ventilation (HVT). Analyzed using Mann-Whitney test. Data in A-D display median, and error bars represent IQR.

Figure 15 shows representative images of the observed histopathology. This demonstrates the mild reduction in perivascular oedema (Figure 15B) and interstitial inflammatory cell infiltration (Figure 15D) in the lung tissue of Trimodulin-treated mice after HVT ventilation compared to control mice.

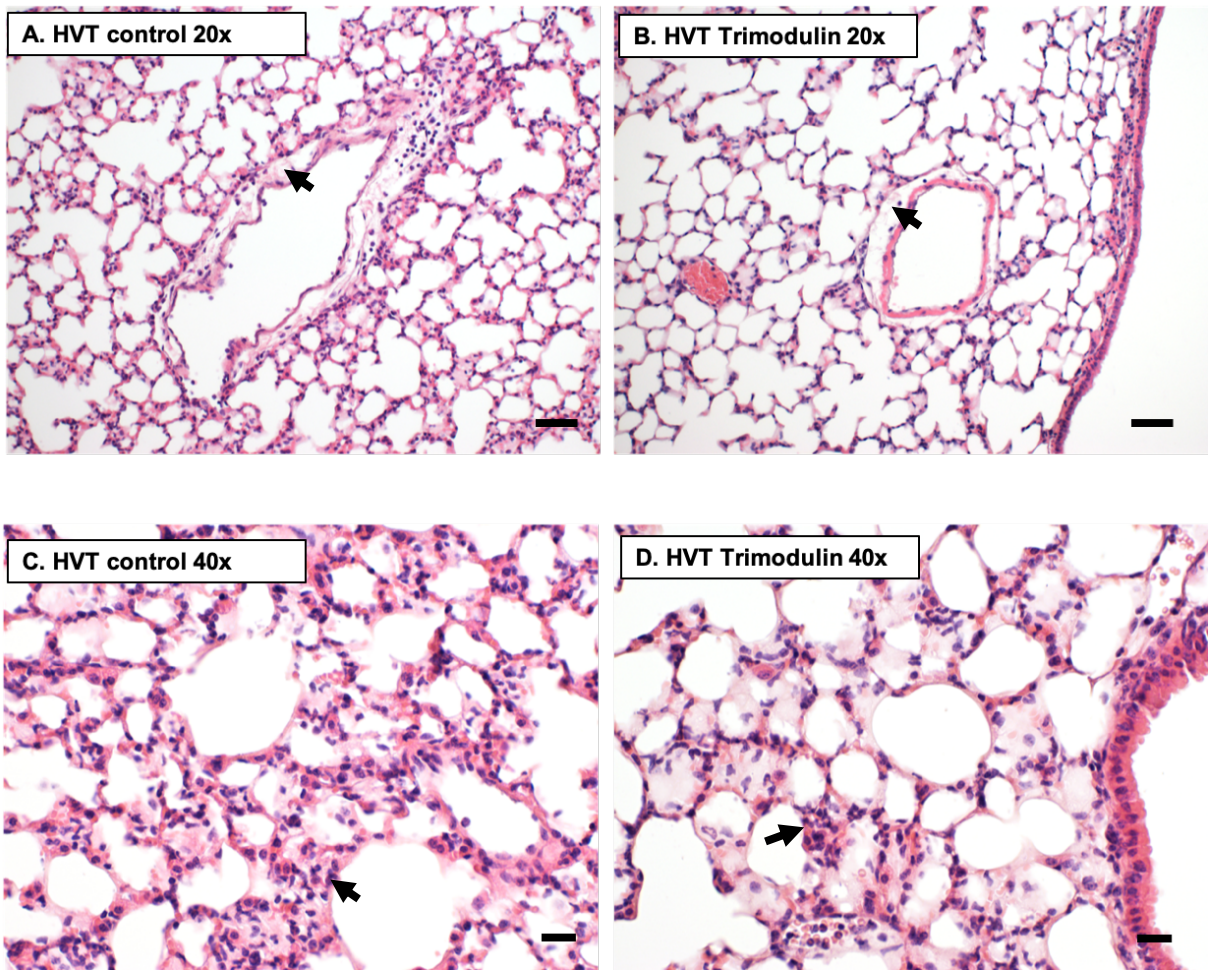

Figure 15. Histopathology of control and Trimodulin-treated mice. Representative lung tissue images stained with H&E stain at various magnifications of light microscopy. **A** – magnification 20x of lung tissue sample of control mouse after 4 hours of high tidal volume (HVT) ventilation showing perivascular oedema (arrow). Scale (line) = 50 μm. **B** – magnification 20x of lung tissue sample of Trimodulin-treated mouse after 4 hours of high tidal volume (HVT) ventilation showing perivascular oedema (arrow). Scale (line) = 50 μm. **C** – magnification 40x of lung tissue sample of control mouse after 4 hours of high tidal volume (HVT) ventilation showing inflammatory cell infiltration into the interstitium (arrow). Scale (line) = 20 μm. **D** – magnification 40x of lung tissue sample of Trimodulin-treated mouse after 4 hours of high tidal volume (HVT) ventilation showing inflammatory cell infiltration into the interstitium (arrow). Scale (line) = 20 μm.

Periodic-acid Schiff (PAS) staining demonstrated no statistical difference in hyaline membrane infiltration (results shown in Figure 14B) with either Trimodulin or control treatment after HVT ventilation (images shown in Figure 16).

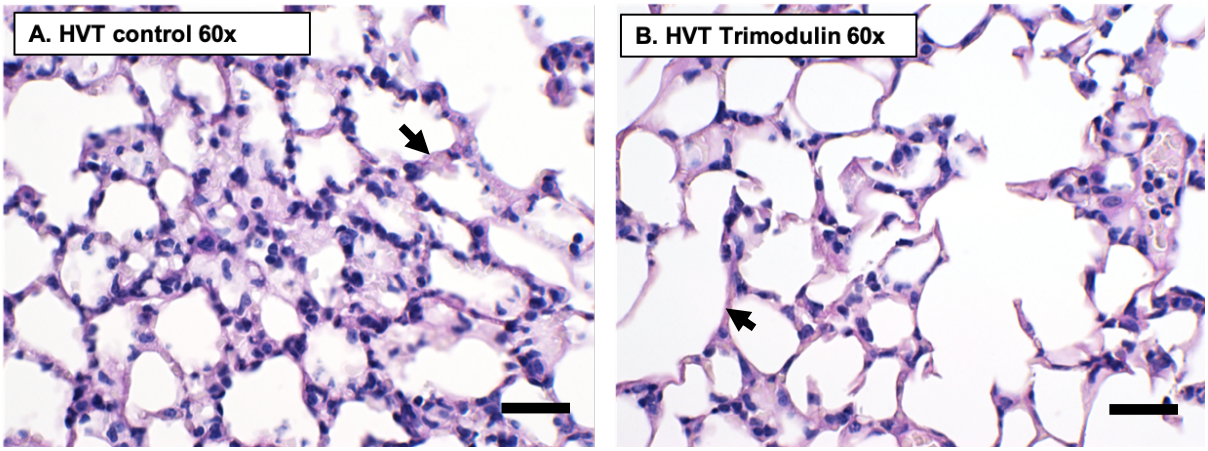

Figure 16. Non-significant difference in histological imaging with PAS staining between control and Trimodulin-treated mice. Representative lung tissue samples stained with PAS stain. **A** – magnification 60x of sample of control mouse after 4 hours of high tidal volume (HVT) ventilation showing hyaline membrane infiltration (arrow). Scale (line) = 20 μm. **B** – magnification 60x of sample of Trimodulin-treated mouse after 4 hours of high tidal volume (HVT) ventilation showing hyaline membrane infiltration (arrow). Scale (line) = 20 μm.

8.3. Local/Systemic Immune Cell Responses and Haematological Parameters

Leucocyte populations have a varied role in the balance of pro- and anti-inflammatory effects that mediate the extent of damage caused by VILI. The study sought to examine further which leucocyte populations were present in the lungs and whether they were affected by Trimodulin or not and pair this knowledge with a haematological analysis of leucocytes in the circulation using the Scil Vet abc™ Animal Blood Counter.

Mice were sacrificed after the termination of ventilation, blood drawn for haematological analysis, cells isolated from BAL and lung samples were taken for flow cytometric analysis of leucocyte populations.

8.3.1. Haematological profiles in either NV or HVT ventilation remained similar

There was no difference in the total number of leucocytes (LEU) between the NV and HVT groups, nor between the control and Trimodulin-treated mice. There was a general increase in the relative number of eosinophils, granulocytes and monocytes (which in the case of monocytes was significant ($P < 0.001$) between the NV and HVT control groups, showing increased inflammation) and a general decrease in the relative number of lymphocytes in the HVT group compared to the NV group. There was also a non-significant tendency for reduced relative eosinophil and monocyte proportions in the Trimodulin-treated group with HVT ventilation (Figure 17).

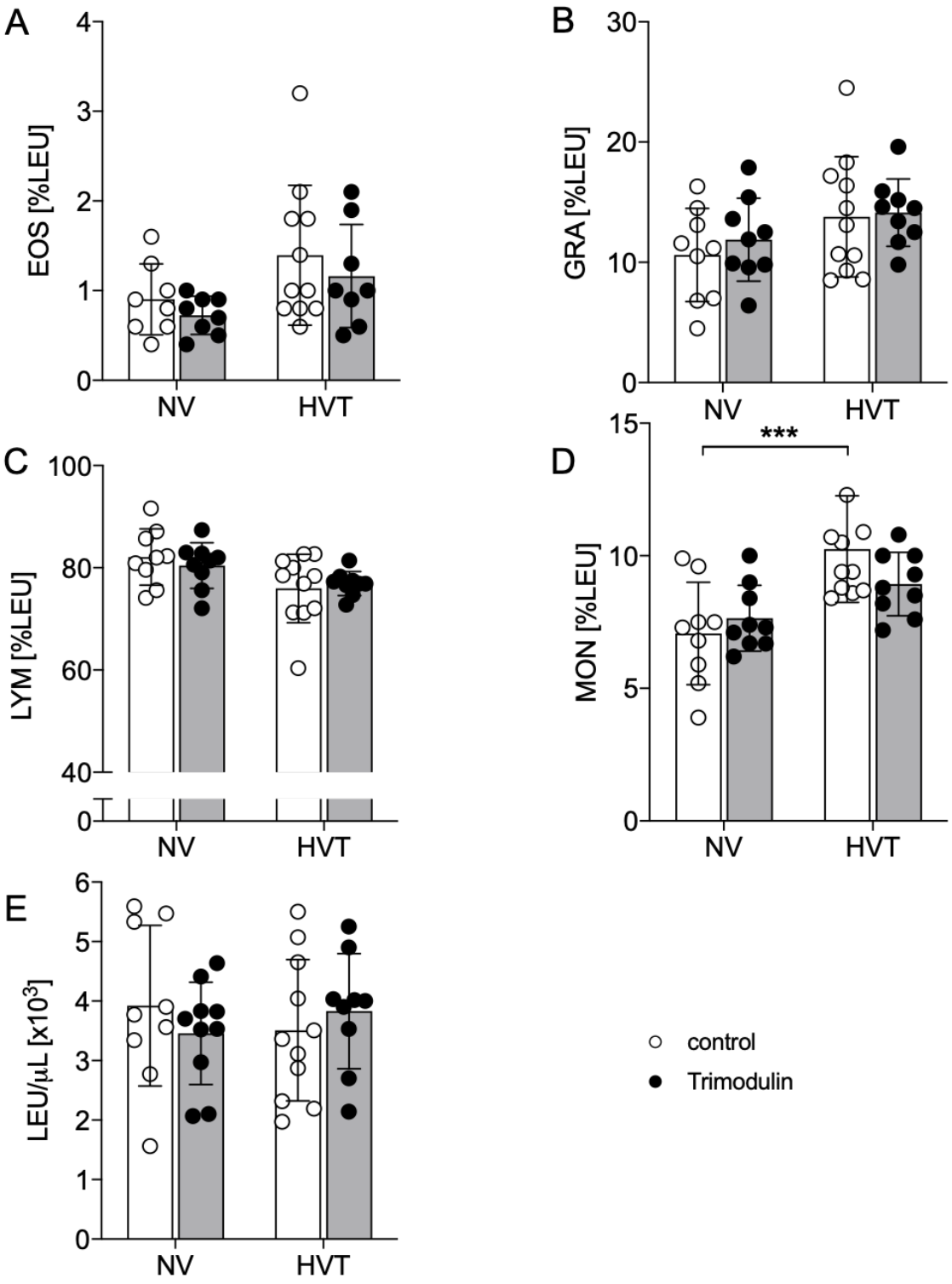

Figure 17. No difference in haematological profile between control and Trimodulin-treated mice. **A** – relative number of eosinophils (EOS) as a percentage of leucocytes (%LEU), **B** - relative number of granulocytes (GRA) as a percentage of leucocytes (%LEU), **C** – relative number of lymphocytes (LYM) as a percentage of leucocytes (%LEU), **D** - relative number of monocytes (MON) as a percentage of leucocytes (%LEU), **E** – absolute number of leucocytes (LEU) in blood after no ventilation (NV) or 4 hours of high tidal volume ventilation (HVT). An asterisk (*) denotes statistical difference between NV and HVT groups, analyzed using two-way ANOVA/Tukey's multiple comparisons test. *** denotes $P < 0.001$. Data in A-E display mean, and error bars represent SEM.

Consumption of haematological products can be evidence of an inflammatory process, but there was no statistical difference detected in red blood cells (RBC), red blood cell distribution width (RDW), haematocrit (HCT) or haemoglobin (HGB) between NV or the HVT groups, nor between the control and Trimodulin-treated mice (Figure 18).

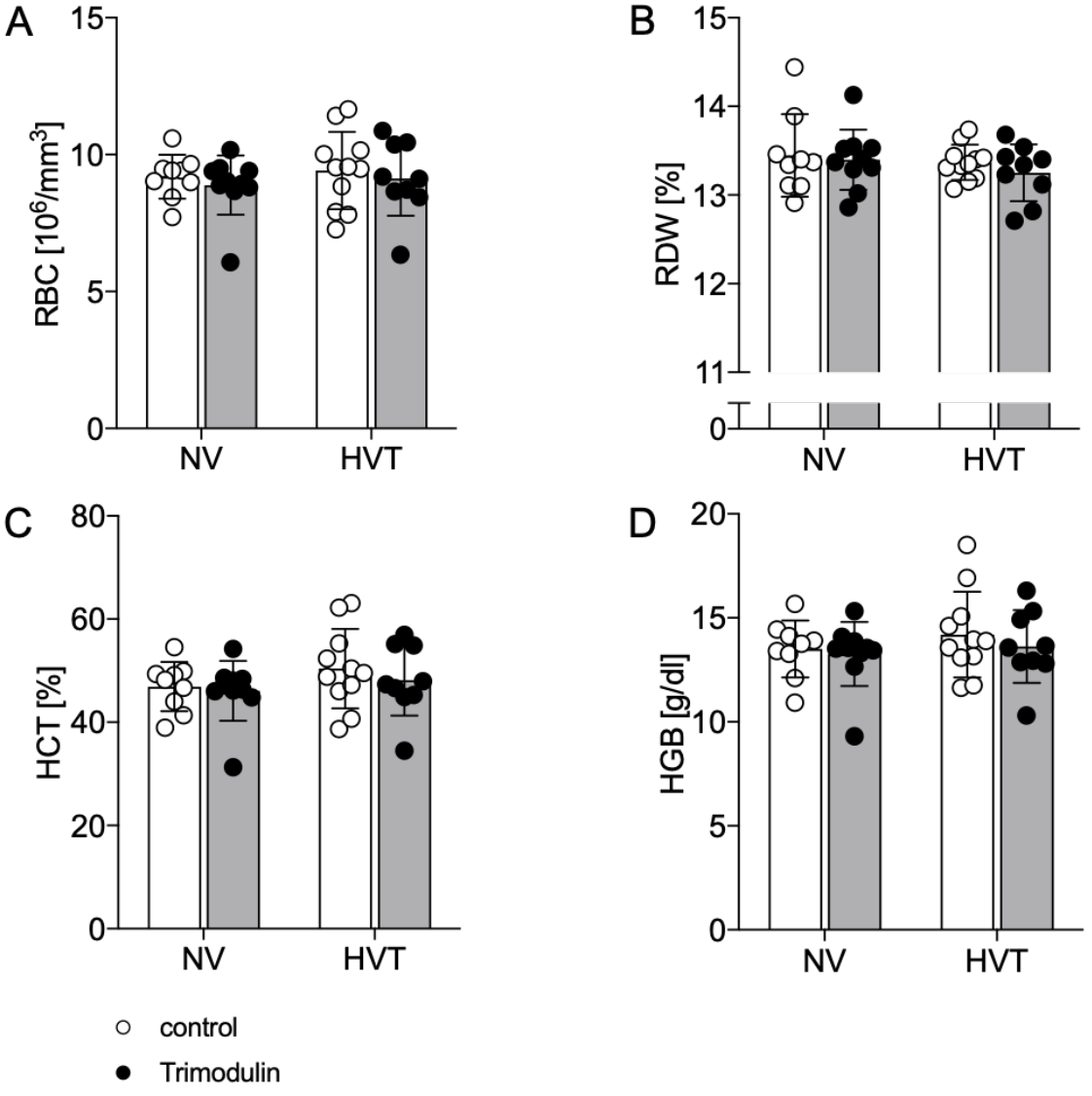

Figure 18. No difference in haematological profiles between control and Trimodulin-treated mice. **A** – absolute number of red blood cells (RBC), **B** – red blood cell distribution width (RDW), **C** – haematocrit (HCT), **D** – haemoglobin (HGB) in blood after no ventilation (NV) or 4 hours of high tidal volume ventilation (HVT). Analyzed using two-way ANOVA/Tukey's multiple comparisons test. Data in A-D display mean, and error bars represent SEM.

Nor was there a difference in other haematological parameters. But there was a general trend towards decreased platelets and a significant increase ($P < 0.05$) in mean platelet volume (MPV) in the HVT group (Figure 19). This likely reflects a systemic response to inflammation.

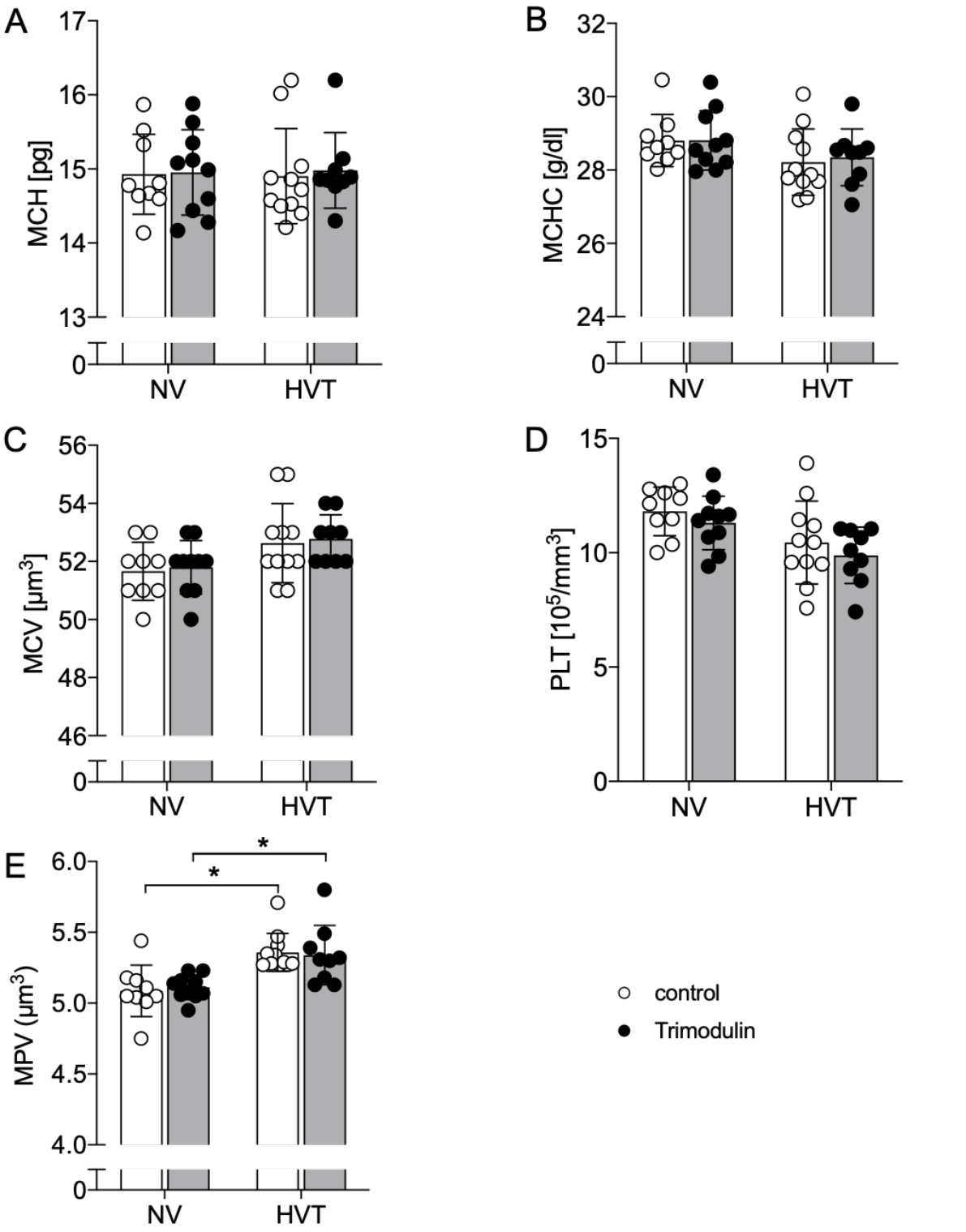

Figure 19. No difference in corpuscular and platelet volumes between control and Trimodulin-treated mice. A – mean corpuscular haemoglobin (MCH), **B** – mean corpuscular haemoglobin concentration (MCHC), **C** – mean corpuscular volume (MCV), **D** – absolute number of platelets (PLT), **E** – mean platelet volume (MPV) in blood after no ventilation (NV) or 4 hours of high tidal volume ventilation (HVT). An asterisk (*) denotes statistical difference between NV and HVT groups, analyzed using two-way ANOVA/Tukey's multiple comparisons test. * denotes $P < 0.05$. Data in A-E display mean, and error bars represent SEM.

8.3.2. Neutrophil infiltration into alveolar spaces is reduced upon Trimodulin treatment

There was a statistically significant reduction ($P < 0.05$) in the relative number of neutrophils (PMNs) found amongst BAL leucocytes after 4 hours of HVT ventilation in Trimodulin-treated mice compared to control mice (Figure 20). There was also a non-significant trend towards a reduction in absolute numbers of PMNs in Trimodulin-treated mice. This implies recruitment of neutrophils to the site of inflammation is diminished with Trimodulin treatment.

As expected, there was significant recruitment of neutrophils to the alveoli with HVT ventilation when compared to NV ventilation ($P < 0.0001$). There was virtually no infiltration of PMNs in NV mice.

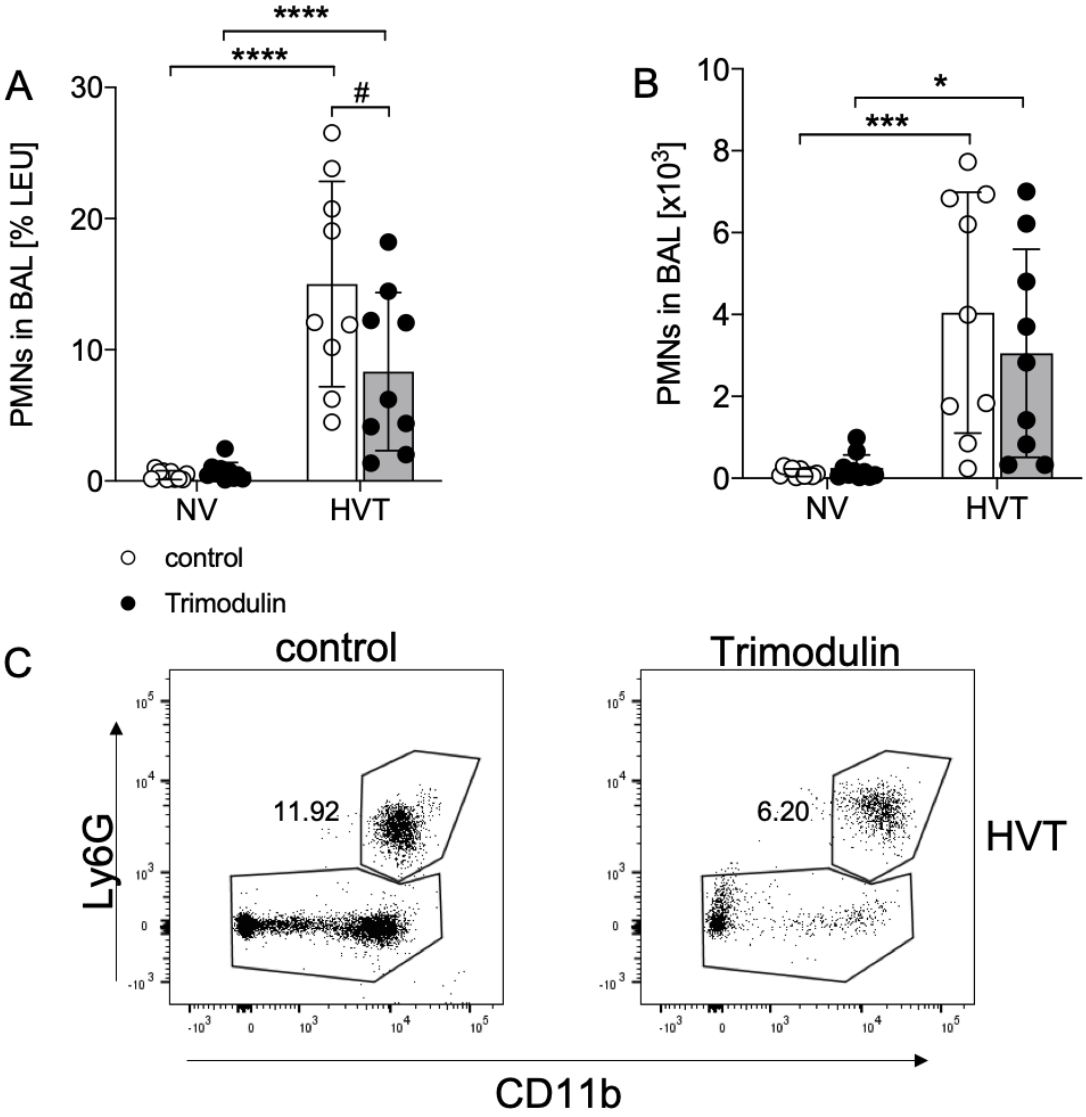

Figure 20. Reduced neutrophil infiltration in the BAL of Trimodulin-treated mice compared to controls. **A** - relative number, **B** - absolute number and **C** - dot plot of polymorphonuclear neutrophils (PMNs) in BAL after 4 hours of high tidal volume ventilation (HVT) in the control group and Trimodulin-treated group. A hashtag (#) denotes statistical difference between control and Trimodulin-treated mice. An asterisk (*) denotes statistical difference between NV and HVT groups, analyzed using two-way ANOVA/Tukey's multiple comparisons test. # denotes P < 0.05. * denotes P < 0.05. *** denotes P < 0.001. **** denotes P < 0.0001. Data in A-B display mean, and error bars represent SEM.

8.3.3. Leucocyte populations besides neutrophils do not change with Trimodulin treatment

Generally, there was no significant difference in the absolute numbers of alveolar macrophages (AMs), inflammatory macrophage/monocytes (IMs) or dendritic cells (DMs) in the alveolar spaces between Trimodulin-treated and control mice.

There was a significant difference between the relative AM populations between the NV and HVT in both control and Trimodulin-treated groups ($P < 0.0001$) which highlights the shift of the inflammatory cellular population caused by VILI. There was a trend towards increased relative numbers of AMs in Trimodulin-treated mice in HVT, suggesting less of a shift to other cellular populations, but this was not statistically significant.

Furthermore, there was a significant difference in IMs between HVT and NV in the control group ($P < 0.001$) although no significant difference was observed between HVT and NV in the Trimodulin-treated group. We noted this pattern also in the haematological profiles of these groups. This indicates the degree of inflammation in the Trimodulin-treated groups is diminished in comparison. There was also a trend towards decreased relative numbers of DCs in the Trimodulin-treated compared to control mice after HVT, but this was not statistically significant (Figure 21).

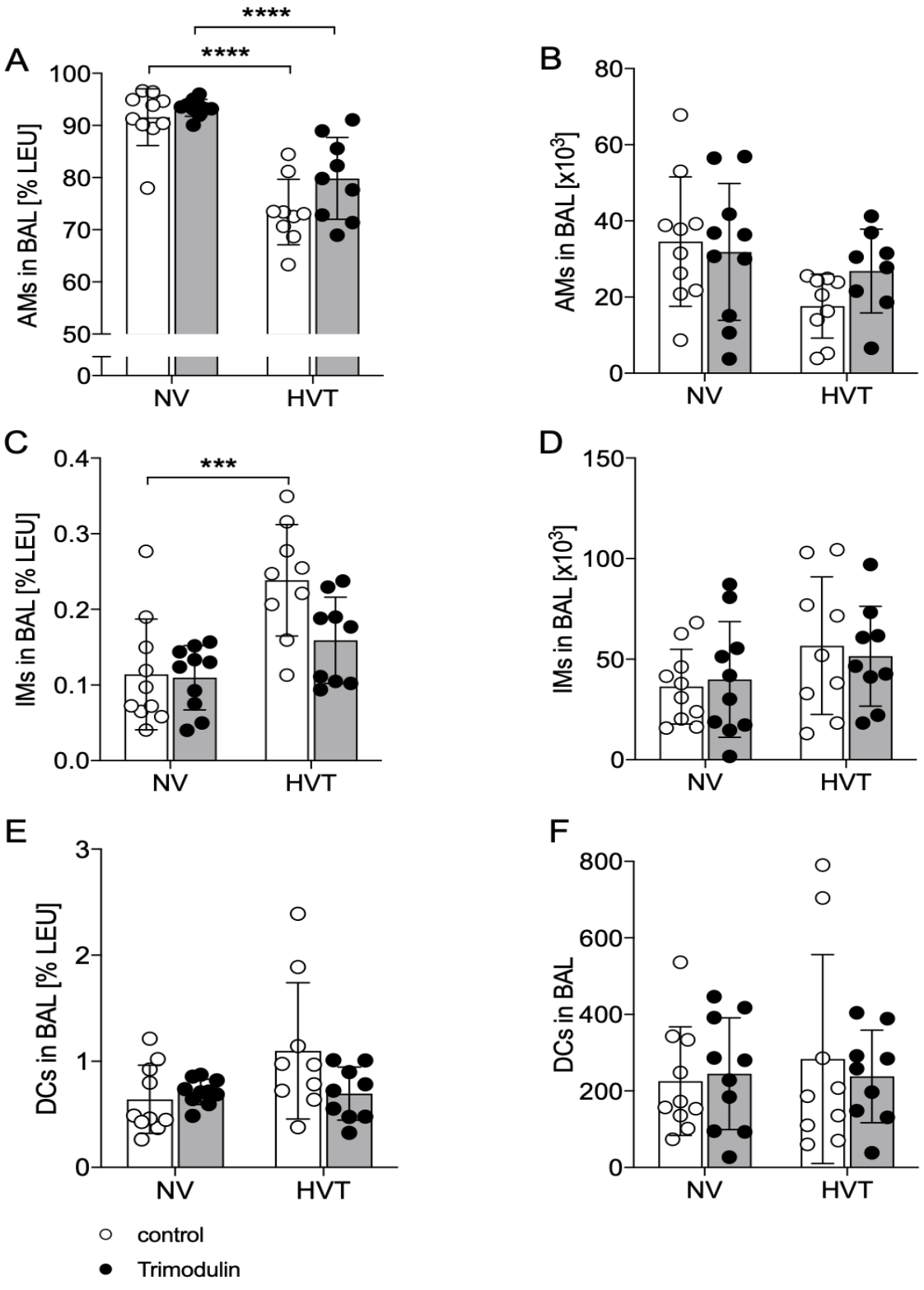

Figure 21. No difference in other cell populations in BAL between control and Trimodulin-treated mice. A - relative number and **B** - absolute number of alveolar macrophages (AMs), **C** - relative number and **D** - absolute number of inflammatory macrophages (IMs), **E** - relative number and **F** - absolute number of dendritic cells (DCs) in BAL after no ventilation (NV) or 4 hours of high tidal volume ventilation (HVT). An asterisk (*) denotes statistical difference between NV and HVT groups, analyzed using two-way ANOVA/Tukey's multiple comparisons test. *** denotes $P < 0.001$. **** denotes $P < 0.0001$. Data in A-F display mean, and error bars represent SEM.

8.3.4. Pulmonary resident and recruited leucocytes populations are unchanged after Trimodulin treatment

There was no significant difference in the absolute or relative numbers of PMNs or AMs in lung homogenate (LH) (Figure 22).

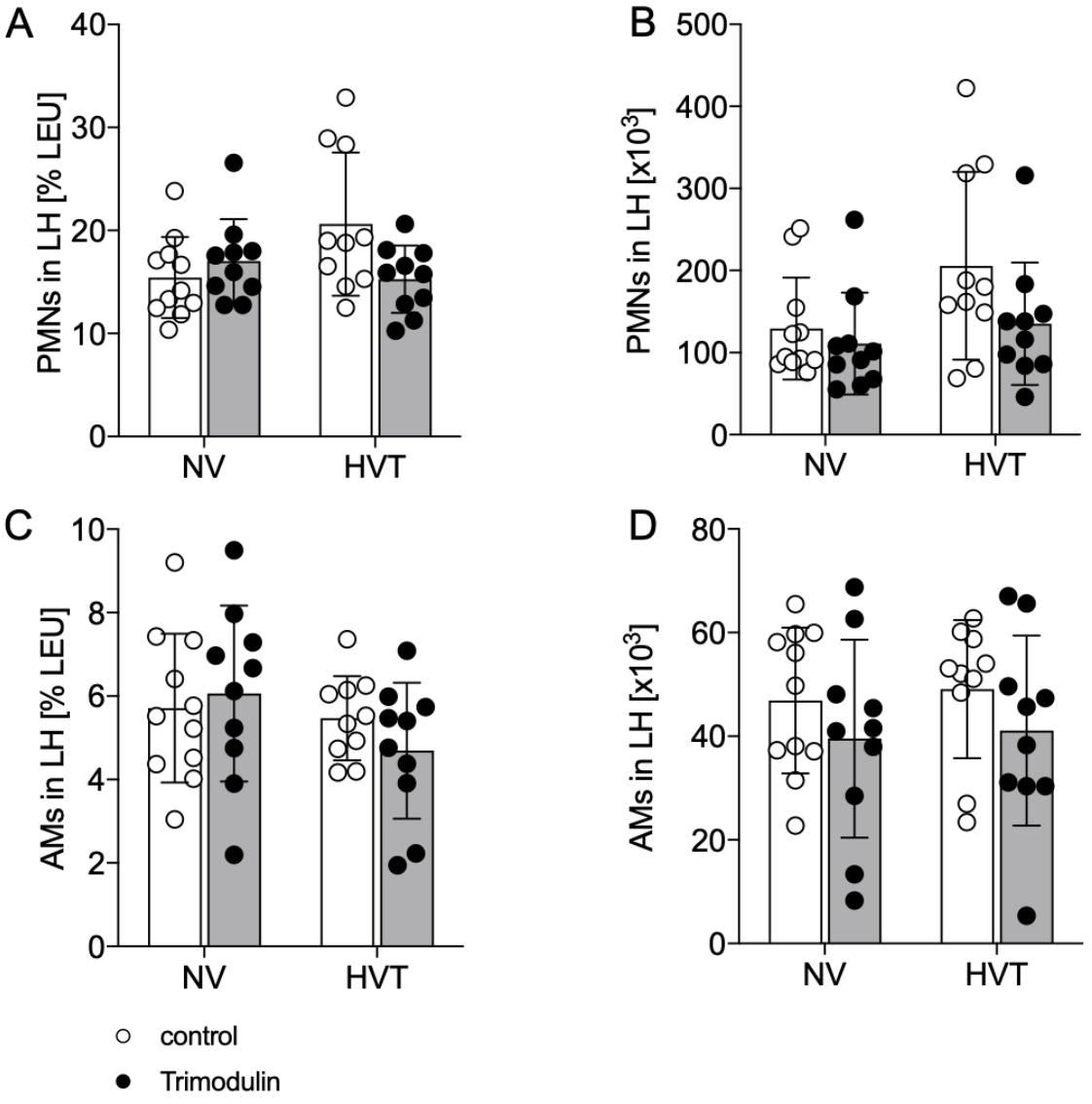

Figure 22. No difference in polymorphonuclear neutrophil or alveolar macrophage populations between control and Trimodulin-treated mice. A - relative number to leucocytes and **B** - absolute number of polymorphonuclear neutrophils (PMNs), **C** - relative number to leucocytes and **D** - absolute number of alveolar macrophages (AMs) in lung homogenate after no ventilation (NV) or 4 hours of high tidal volume ventilation (HVT). Analyzed using two-way ANOVA/Tukey's multiple comparisons test. Data in A-D display mean, and error bars represent SEM.

There was a significant increase in the relative ($P < 0.0001$) and absolute ($P < 0.001$) numbers of IMs in LH in the HVT group compared to the NV group. Within this HVT group, there was a tendency towards reduced relative and absolute numbers of IMs in the Trimodulin-treated mice compared to the control mice. A similar trend was observed in DCs too. Overall, this represents a shift to reduced inflammation upon Trimodulin treatment. However, this trend was not statistically significant (Figure 23).

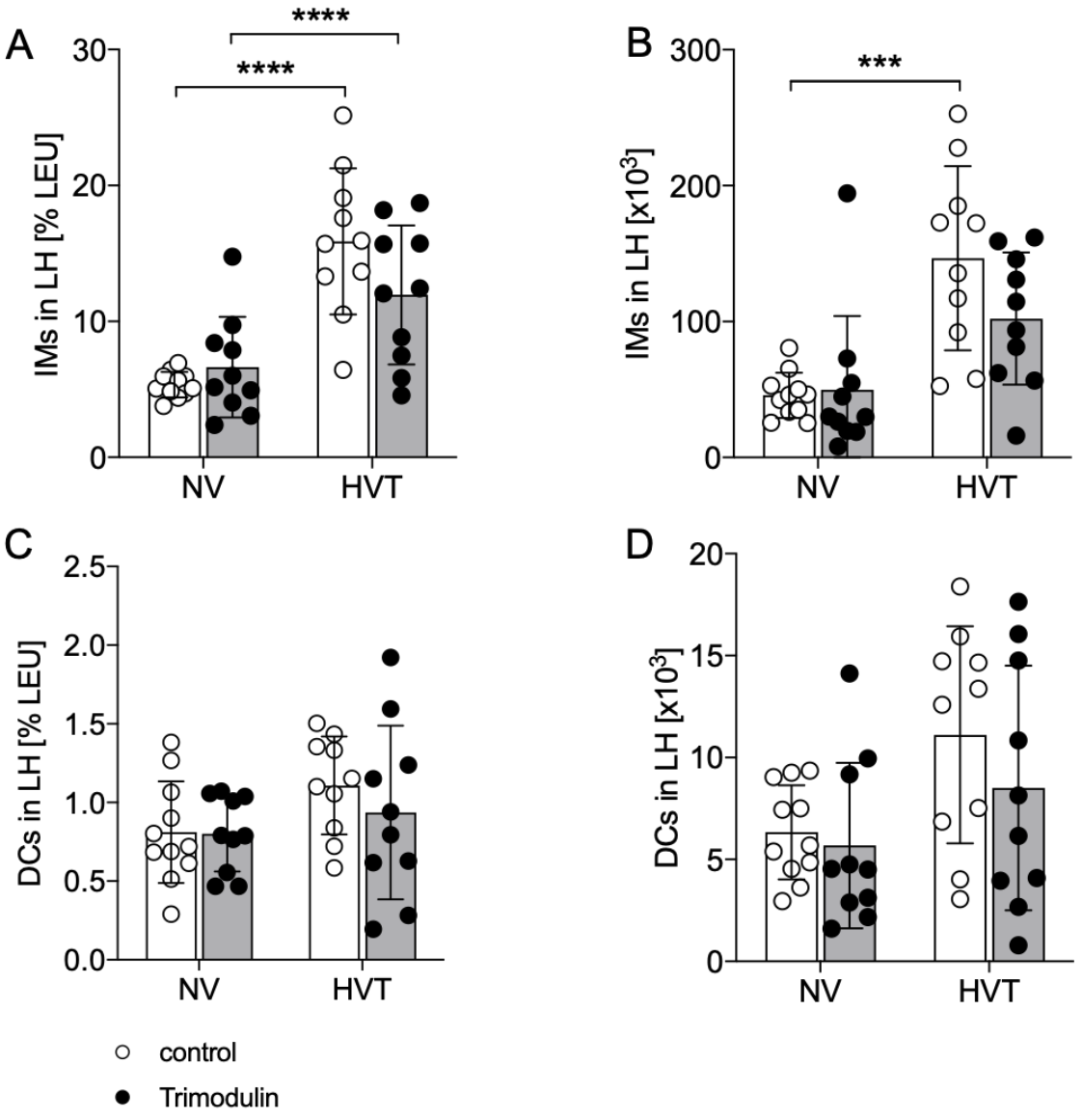

Figure 23. No difference in inflammatory macrophage or dendritic cell populations between control and Trimodulin-treated mice. A - relative number to leucocytes and **B** - absolute number of inflammatory macrophages (IMs), **C** - relative number to leucocytes and **D** - absolute number of dendritic cells (DCs) in lung homogenate after no ventilation (NV) or 4 hours of high tidal volume ventilation (HVT). An asterisk (*) denotes statistical difference between NV and HVT groups, analyzed using two-way ANOVA/Tukey's multiple comparisons test. *** denotes P < 0.001. **** denotes P < 0.0001. Data in A-D display mean, and error bars represent SEM.

8.4. Inflammatory Mediators

In order to establish the effect of Trimodulin on the modulation of lung inflammation concentrations of inflammatory cytokines, chemokines and complement were analyzed.

The pro-inflammatory cytokines TNF-α, IL-1β and IL-6 are important cytokines produced by activated macrophages in response to cellular stress and precipitate a pro-inflammatory milieu. In contrast IL-10 has a largely anti-inflammatory role and is produced to counterbalance the degree of inflammation. Chemokines such as CXCL10 and CCL5 are chemo-attractant to a number of cell types, whereas CXCL1 is more explicitly important to neutrophil recruitment and CCL2 to monocytes. The balance of chemokines and cytokines is important to deducing the cell types and degree of inflammation in either control or Trimodulin-treated groups. Similarly complement activation is essential in certain forms of inflammation too.

8.4.1. Trimodulin treatment did not affect systemic concentrations of inflammatory mediators

There was a significant increase in IL-6 concentrations ($P < 0.001$ and $P < 0.01$, respectively) in the HVT group compared to the NV group. We also noted a mild tendency towards reduced pro-inflammatory IL-6 concentrations in Trimodulin-treated compared to control mice after HVT ventilation. There was also a tendency towards increased anti-inflammatory IL-10 concentrations in Trimodulin-treated compared to control mice after HVT ventilation. Interestingly, the trend towards increased IL-10 concentrations was replicated in both NV ventilated and HVT ventilated mice. However, an increase in pro-inflammatory TNF-α in Trimodulin-treated mice after HVT ventilation was demonstrated (Figure 24). Although, these findings were not significant.

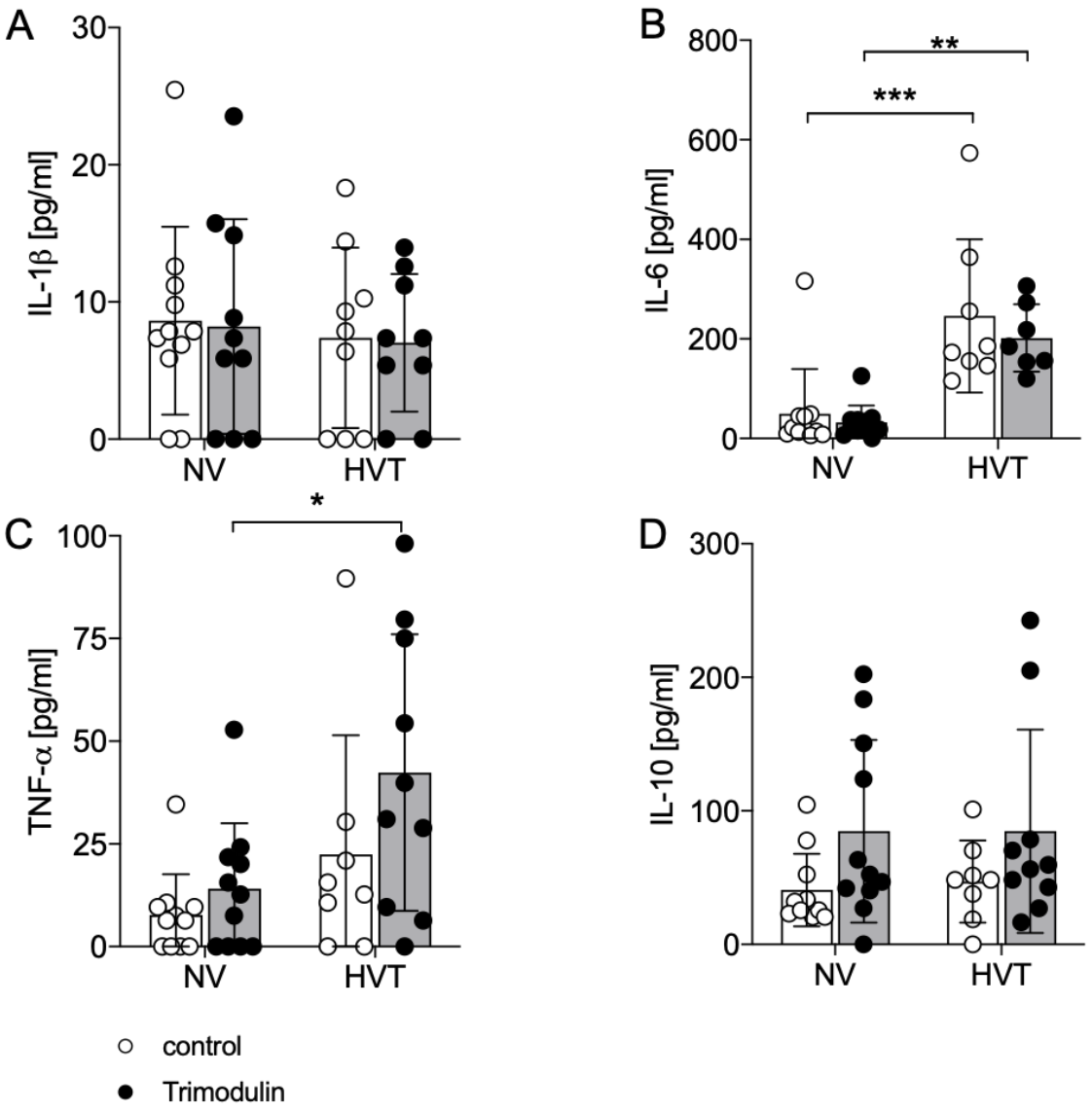

Figure 24. No significant difference in cytokine concentrations between control and Trimodulin-treated mice. A – concentration of IL-1β, **B** - concentration of IL-6, **C** - concentration of TNF-α, **D** - concentration of IL-10 in plasma after no ventilation (NV) or 4 hours of high tidal volume ventilation (HVT). An asterisk (*) denotes statistical difference between NV and HVT groups, analyzed using two-way ANOVA/Tukey's multiple comparisons test. * denotes $P < 0.05$. ** denotes $P < 0.01$. *** denotes $P < 0.001$. Data in A-D display mean, and error bars represent SEM.

There were significant increases in chemokine concentrations of CXCL10 (specific to Trimodulin-treated mice), CXCL1 and CCL2 after HVT ventilation compared to NV ventilation. There was tendency towards reduced pro-inflammatory CXCL1 concentrations in Trimodulin-treated mice compared to control mice after HVT ventilation. Whereas there was a tendency towards increased anti-inflammatory CCL2 and CXCL10 concentrations in Trimodulin-treated mice compared to control mice after HVT ventilation, although in both cases were non-significant (Figure 25).

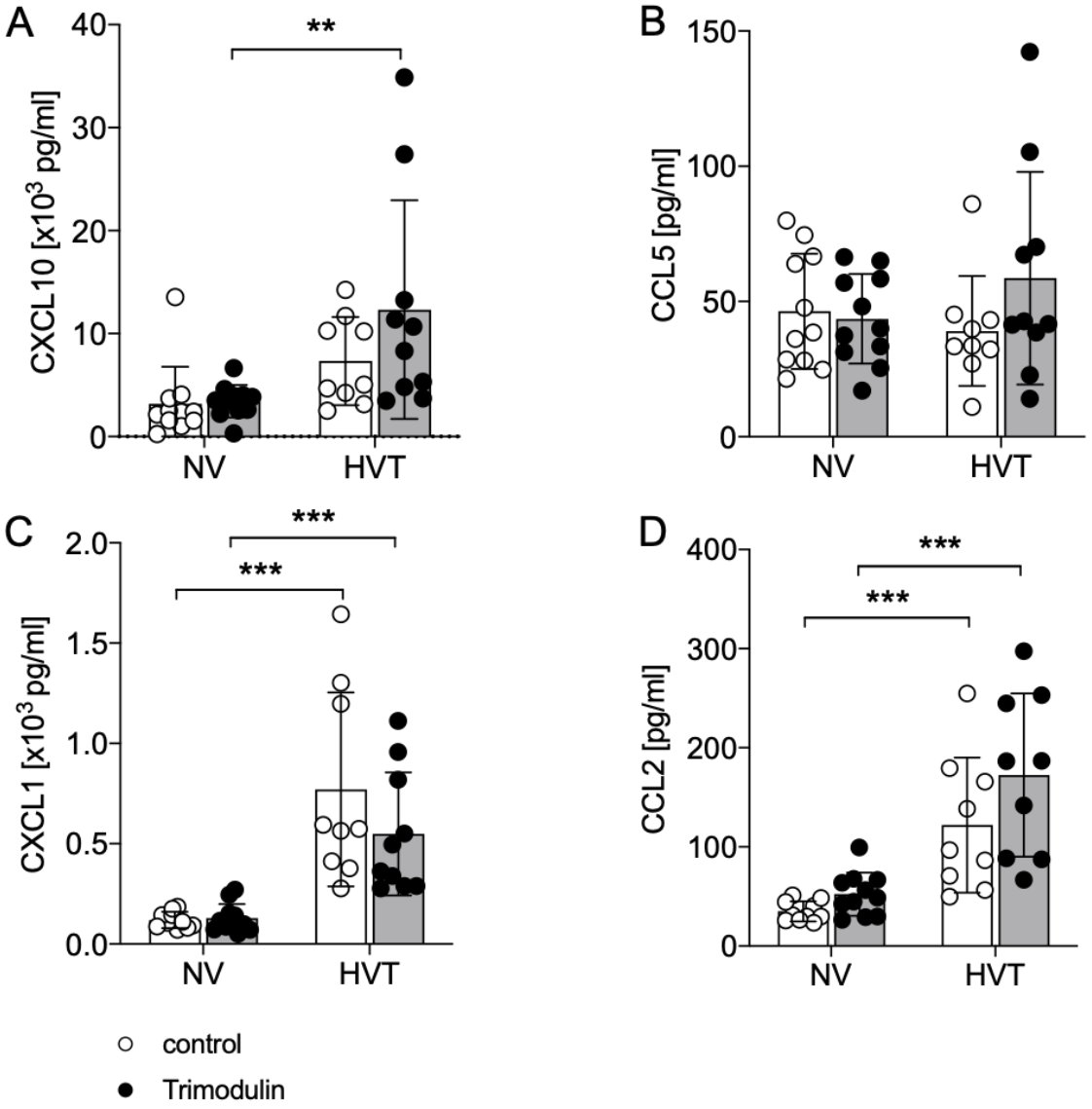

Figure 25. No significant difference in chemokine concentrations between control and Trimodulin treatment. A - concentration of CXCL10, **B** - concentration of CCL5, **C** - concentration of CXCL1, **D** - concentration of CCL2 in plasma after no ventilation (NV) or 4 hours of high tidal volume ventilation (HVT). An asterisk (*) denotes statistical difference between NV and HVT groups, analyzed using two-way ANOVA/Tukey's multiple comparisons test. ** denotes $P < 0.01$. *** denotes $P < 0.001$. Data in A-D display mean, and error bars represent SEM.

8.4.2. Control and Trimodulin-treated mice exhibit comparable complement C5a concentrations in either NV or HVT ventilation

There was no difference in the concentrations of complement C5a in either the NV or HVT ventilated groups. Nor was there a difference in the C5a concentrations between control and Trimodulin-treated mice. This was shown in both plasma (Figure 26A) and BAL samples (Figure 26B). These results taken together suggest there is limited scope for Trimodulin having a role in the regulation of complement activation.

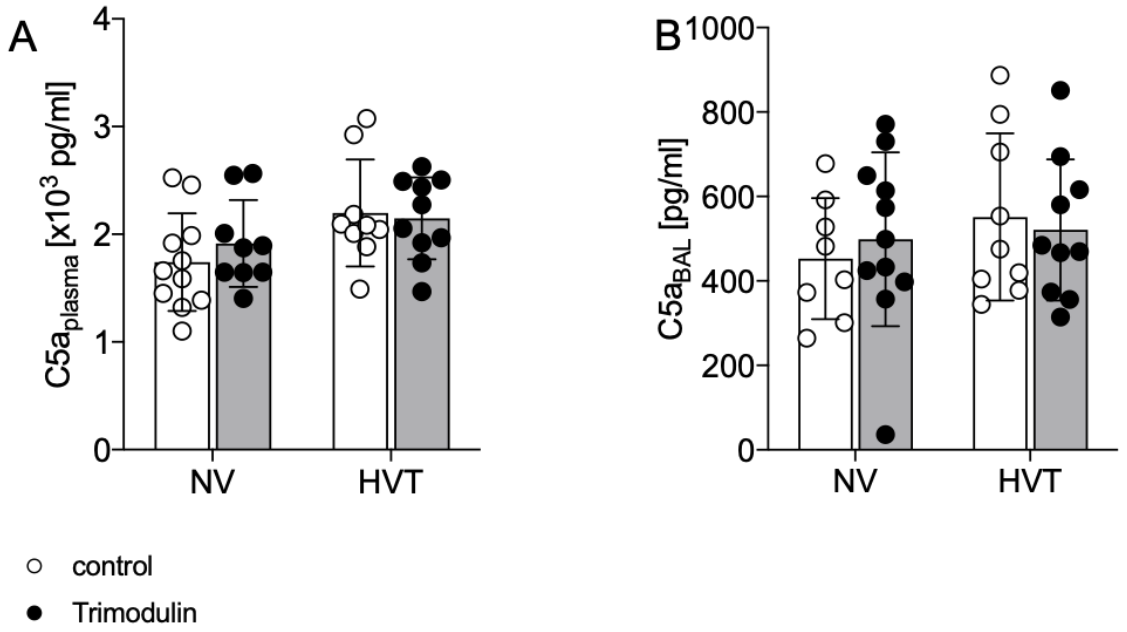

Figure 26. No difference in complement C5a component concentration between control and Trimodulin treatment. A – concentration of C5a in plasma, **B** - concentration of C5a in BAL after no ventilation (NV) or 4 hours of high tidal volume ventilation (HVT). Analyzed using two-way ANOVA/Tukey's multiple comparisons test. Data in A-B display mean, and error bars represent SEM.

9. Discussion

Ventilator-induced lung injury (VILI) is a common complication of sCAP, as a result of the mechanical ventilation that is required to support the respiratory system during the disease process (19). The pathogenesis behind VILI includes both a mechanical component (23) and a biological element (27), whereby host immune response unleashes an inflammatory response that is damaging to the lungs. The recent phase 2 CIGMA trial (73) demonstrated that, in a cohort of ventilated patients with sCAP, Trimodulin (an IgM/IgA-enriched immunoglobulin preparation) treatment has shown benefit in patients with the worst clinical and biochemical parameters. It remains unclear whether Trimodulin is effective on either sCAP or VILI and what the precise mechanism of action is. This project aimed to establish whether Trimodulin was effective in a murine model of VILI without infection (sterile inflammation) and determine how the mechanism of action might operate in this setting. Our results demonstrate that, in the context of VILI, Trimodulin may be beneficial to the subject by limiting the impact of mechanical ventilation on the lungs. This is a consequence of reduced neutrophil infiltration into the alveoli, likely mediated by modulation of the humoral immune response that involves IL-6, IL-10, CXCL1 and CCL2.

Little difference was observed in vital parameters between the control and Trimodulin-treated group during HVT ventilation. The response of steadily reducing blood pressure, increasing heart rate and eventually falling oxygen saturations was observed in both groups upon HVT ventilation and was consistent with what would be expected in patients with VILI. Trimodulin did not appear to improve this picture. These findings are congruent with vital parameters observed in a similar rat model of ARDS where IgM-enriched polyclonal immunoglobulins reduced bacteremia in *Klebsiella pneumoniae* infection (77). In that study the authors noted a similar pattern of mean arterial pressure (MAP) to that which we observed, with no difference between the immunoglobulin-treated group and the control group.

Our data regarding improvements in ventilator parameters after treatment with Trimodulin represent novel findings. We demonstrated a significant reduction in airway opening pressure and elastance together with a significant improvement in compliance. Whilst we did not observe statistically significant reductions in

inflammation and permeability, there was a trend towards their reduction. Thus, there is likely a summative effect manifesting in improvements in ventilation parameters. Our findings would correspond with an improvement in clinical status (78, 79), where more compliant lungs require lower pressures to ventilate them, thereby minimizing mechanical stress. This research group has previously shown that the ventilation parameters measured in the untreated control group (80) result in significant lung injury. So, we can be confident that improving these parameters would mitigate the extent of this injury. In the context of treatment with IgM/IgA-enriched polyvalent immunoglobulin preparations, this would be the first time that it has been shown there is a significant improvement in ventilator parameters.

Arterial blood gas analysis demonstrated no difference in PaO_2 and $PaCO_2$ values between control and Trimodulin-treated mice after 4 hours of HVT ventilation. This implies that there was not a significant breakdown of the alveolar-capillary barrier so as to impair gaseous exchange, within the time constraints of this study. This is concordant with results found in a study by Vaschetto et al. (81), in which they ventilated Sprague-Dawley rats for 3.5 hours after intratracheal instillation of LPS with or without Pentaglobin (PNT), another IgM-enriched polyvalent immunoglobulin preparation. The authors also found a decrease in PaO_2 after HVT but no difference in the oxygenation status of either the LPS or LPS + PNT groups. Similarly, this study also tried to quantify changes in lung permeability by determining wet-dry lung ratios. They found that whilst there was an increase in permeability compared to controls there was no difference between the LPS and LPS + PNT groups. This is consistent with our results, which showed a moderate trend towards reduced alveolar permeability of Trimodulin-treated mice compared to the control HVT group, but without statistical significance. These results also support our findings that Trimodulin has a limited impact on reducing the impairment of the alveolar-capillary barrier and gaseous exchange, and as histopathology suggested, little effect on mitigating the extent of lung damage caused by VILI.

In order to establish the mechanism by which Trimodulin functions, flow cytometry analysis was performed. We determined the composition of the cell populations in broncho-alveolar lavage (BAL) and lung homogenate (LH) and deduced the migration

patterns of the inflammatory cells involved in VILI. There was a significant reduction in the number of neutrophils found in the alveolar spaces of mice treated with Trimodulin compared to control mice who also underwent the HVT ventilation protocol. The implication of this is that Trimodulin reduces translocation of neutrophils into the alveolar compartment. Thereby, it could be expected that there would be a reduction in lung injury as previous studies have correlated increased neutrophil proteinase and oxidant activity in the alveoli with more severe damage (46).

Although there was a trend towards reducing inflammatory macrophage/monocyte populations in both the alveolar space and lung tissue, no significant difference was found in other cellular populations between the groups. This was consistent with haematological analysis of arterial blood, which exhibited a non-significant reduction in monocytes too. This phenomena of reduction in neutrophil recruitment was also observed by Barrat-Due et al. (82). They investigated the response of mechanically ventilated pigs treated with Pentaglobin to *Escherichia coli* infection. Their data demonstrates a significant reduction in neutrophil counts in the plasma after 60 minutes of ventilation (and persisting for the total 240 minutes of the procedure) when compared to untreated controls. They did not conclude that this reduction in neutrophils was necessarily important to the mechanism of action, but it is of interest that both our studies have recognized this. In terms of the other cell populations there is a paucity of research into their roles in the context of polyclonal immunoglobulin treatment in mechanical ventilation and so our findings cannot be compared to current literature.

Given the findings of alterations in the composition of cell populations with Trimodulin, this study sought to investigate its effect on the cytokine and chemokine profile. There was no significant difference in cytokine or chemokine concentrations between the control and Trimodulin-treated mice after HVT ventilation. However, it is important to note that whilst we did not observe any significant differences in cytokine concentrations in plasma there was evidence of a tendency towards reduced IL-6 and increased IL-10 concentrations in the Trimodulin-treated mice compared to the control mice. This would be in keeping with a shift from a pro-inflammatory to a more anti-inflammatory environment. Conversely, we did observe a non-significant increase in pro-inflammatory cytokine TNF-α in the Trimodulin-treated group.

These findings are of interest because the literature is conflicted with regard to the effect of IgM-enriched polyvalent immunoglobulin preparations on inflammatory cytokines, although it is more consistently established in the context of IVIg (83). Shmygalev et al. (84) addressed the effect of Trimodulin in a rabbit model of endotoxemia and severe sepsis and observed no difference in the concentrations of IL-1, IL-6 and TNF-α. In contrast, Barrat-Due et al. (82) found reduced IL-6 and normal TNF-α levels after treatment with polyclonal immunoglobulins. They propose this suggest IgM-enriched polyvalent immunoglobulins modulate the immune system by causing a shift to an anti-inflammatory environment although there is no considerable impact on lung damage. Vaschetto et al. (81) found increased concentrations of anti-inflammatory IL-10 and significantly reduced levels of pro-inflammatory TNF-α cytokines.

Given this debate it is reasonable to presume that modulation of cytokine activity varies between different animal models and may not be easily compared. Also, our findings of increased TNF-α, whilst not significant, do diverge with the current literature. Whilst this may be specific to our mouse model, it must also be recognized that the concentrations of TNF-α measured were very small and caution must be taken, that such small concentrations may carry a certain error with their measurement.

It is also worth noting, that there was no increase in concentrations of complement component C5a after HVT ventilation in either Trimodulin-treated or control mice. Rieben et al. (85) used *in vitro* experiments to demonstrate that Pentaglobin treatment induced inhibition of deposition of C1q, C4 and C3 in the classical complement pathway. They subsequently showed in a rat model of nephritis that C3, C6 and C5b-9 deposition in the rat glomeruli was reduced upon Pentaglobin treatment. Unfortunately, they did not comment on C5a concentrations and so we are unable to compare our data and make inferences regarding the role of polyclonal immunoglobulins in the activation of complement. However, these findings give us scope to expand upon our current work to establish a precise mechanism of action.

Taken together, based on our data we speculate that Trimodulin functions by shifting the composition of cytokines to a more anti-inflammatory milieu. Increased levels of anti-inflammatory cytokines such as IL-10 inhibit the NF-κB-mediated stimulation of pro-inflammatory cytokines such as IL-6. Consequently, there are fewer chemotactic signals to recruit leucocytes (predominantly neutrophils) to the alveoli and so there is less inflammation and reduced permeability of the alveolar-capillary membrane. Although not all of this have been shown to be of statistical significance, their cumulative effect might be that the integrity of the alveoli is better maintained, so compliance is improved and lower ventilatory pressures are required. Further studies are required to consolidate and refine this model.

IVIg is already used clinically as a treatment for a number of autoimmune conditions. One review (86) focusing on idiopathic thrombocytopenic purpura (ITP) highlighted the importance of IgG antibody in activating Fcγ receptors that are associated with attenuating activation pathways. This has been shown to promote production of the immunosuppressant cytokine IL-10 in murine models (83). As we observed a tendency to increased IL-10 production with Trimodulin administration, a plausible mechanism may be via interaction with Fc-receptors. Although, in the murine model these will differ.

Furthermore, IVIg administration has been shown to downregulate transcription of pro-inflammatory cytokines and chemokines. Xu et al. (87) showed that IVIg works to reduce mRNA transcription of the cytokine IL-6. They theorized that IVIg contains soluble receptors which “soak up” upstream TNF-α or IL-1β, stimulators of IL-6 production. This provides support for our demonstration of reduced quantities of downstream effector molecules such as IL-6. There is a resultant shift to an anti-inflammatory milieu, therefore decreasing leucocyte infiltration to the affected region.

Another element to consider in the potential mechanism of action of Trimodulin, is the effect it has on DAMPs. High Mobility Group Box-1 (HMGB-1) protein is widely recognized as an important signaling molecule released during sepsis (88). Administration of high doses-IgG was shown to reduce HMGB-1 concentration and inhibit its activity in a rat model of sepsis (89). Given the high concentrations of IgG and IgM in Trimodulin, it is reasonable to assert that this may reduce DAMP activity in

our model of VILI. The importance of DAMPs to the NLRP3 inflammasome model of inflammation in VILI has already been outlined. Therefore, DAMP regulation may also provide another mechanism that adds to the summative action of Trimodulin.

Further *in vitro* cell stretch experiments to measure the concentration of DAMPs in lung endothelial cells could elucidate this. The FLEXCELL Tension Plus System (Flexcell International, USA) is used to expose seeded endothelial or epithelial cells to cyclic stretch that correspond to the pressures exerted by mechanical ventilation and can then use a proximity ligation assay to measure the concentration of DAMPs produced (90). Utilizing this technique would give us a better understanding of the effect Trimodulin has on DAMP activity after cyclical cell stretch.

Whilst there was some suggestion of reduction in alveolar barrier injury in the histopathological studies in the Trimodulin-treated group compared to the control group, this was not significant. However, immunofluorescent electron microscopy of the barrier junction could better characterize more subtle differences observed in permeability between the groups.

Finally, the CIGMA trial studied the effects of Trimodulin in mechanically ventilated patients with sCAP. Whilst we have established the quantitative effect of Trimodulin on subjects in sterile conditions with mechanical ventilation, the effect of bacterial infection has not been accounted for. There are multiple potential mechanisms of action by which Trimodulin may work with regards to direct interaction with a bacterial infection. It has been shown, for instance, that the naturally occurring antibody IgM binds capsular pneumococcal polysaccharides and phosphorylcholine (91). In an IgM/IgA-enriched preparation such as Trimodulin, a significant portion of the anti-inflammatory effect observed in the CIGMA trial may be mediated by binding of foreign antigens as opposed to cytokine or chemokine targets. Consequently, the full extent of the effect of Trimodulin may not have been realized in a sterile model such as ours. Therefore, further arms of this study will assess the effect of Trimodulin in a murine model of *Streptococcus (S.) pneumoniae* and a further model of *S. pneumoniae* and mechanical ventilation. This may reflect the cumulative effect of Trimodulin on both sCAP and VILI.

There are several factors that have to be taken into consideration with this study. Firstly, the ventilation protocol used is different compared to other similar studies in the literature. There are a multitude of small-animal ventilators on the market and we have used one with specific settings that has been established to produce consistent lung injury, so as to best model VILI. Consequently, this means there is limited scope to compare results based on ventilator parameters, but it does give us the opportunity to make general assessments in findings between studies.

To the best of our knowledge, this is the first murine model of VILI assessing the effect of IgM-enriched polyvalent immunoglobulin therapy. There have seen rat, pig and rabbit models already but there are inevitable differences in the physiological and immunological constitution of the subjects which may affect the comparability of results between models. However, such findings do add to the growing body of evidence evaluating the mechanism of action of immunoglobulins.

Lastly, in this model the mice were ventilated for 4 hours. This is a potential limitation as it does not correlate with the clinical setting, where VILI is a summation of lung injury over many days on a ventilator. Therefore, we could be excluding more significant lung inflammation and changes in cell populations that occur later in the process of VILI. However, there is good reason for this protocol because we are able to maximize experimental control of confounding conditions *in vivo* whilst achieving a reliable model of lung injury. Although this may not be reflected clinically, the model can provide enough evidence to consider whether prophylactic adjuvant immunoglobulin therapy may be beneficial.

In conclusion, this study demonstrated a reduction in lung injury in a murine model of VILI when subjects were treated with an IgM/IgA-enriched immunoglobulin adjuvant therapy (Trimodulin). This was correlated to a shift to an anti-inflammatory immunological profile and reduced translocation of neutrophils into the alveolar space. The cumulative effect of this was improvement in lung compliance and reduction in required ventilatory pressures. As some results were inconclusive, further studies are required to elucidate the precise mechanism by which Trimodulin functions.

10. Bibliography

1. Die 10 häufigsten Todesursachen insgesamt. Statistisches Bundesamt: Destatis; 2018 [Available from: https://www.destatis.de/DE/ZahlenFakten/GesellschaftStaat/Gesundheit/Todesursachen/Tabellen/SterbefaelleInsgesamt.html]. Last accessed: 26th October 2018.
2. Kolditz M, Tesch F, Mocke L, Hoffken G, Ewig S, Schmitt J. Burden and risk factors of ambulatory or hospitalized CAP: A population based cohort study. Respir Med. 2016;121:32-8.
3. Ludwig E, Bonanni P, Rohde G, Sayiner A, Torres A. The remaining challenges of pneumococcal disease in adults. Eur Respir Rev. 2012;21(123):57-65.
4. GmbH A-IfaQuFiG. Bundesauswertung zum Erfassungsjahr 2014. PNEU – Ambulant erworbene Pneumonie. Qualitätsindikatoren. 2014.
5. Ewig S, Birkner N, Strauss R, Schaefer E, Pauletzki J, Bischoff H, Schraeder P, Welte T, Hoeffken G. New perspectives on community-acquired pneumonia in 388 406 patients. Results from a nationwide mandatory performance measurement programme in healthcare quality. Thorax. 2009;64(12):1062-9.
6. Koppe U, Suttorp N, Opitz B. Recognition of Streptococcus pneumoniae by the innate immune system. Cell Microbiol. 2012;14(4):460-6.
7. Janeway CA, Jr. Approaching the asymptote? Evolution and revolution in immunology. Cold Spring Harb Symp Quant Biol. 1989;54 Pt 1:1-13.
8. Kono H, Rock KL. How dying cells alert the immune system to danger. Nat Rev Immunol. 2008;8(4):279-89.
9. Opitz B, van Laak V, Eitel J, Suttorp N. Innate immune recognition in infectious and noninfectious diseases of the lung. Am J Respir Crit Care Med. 2010;181(12):1294-309.
10. Marriott HM, Jackson LE, Wilkinson TS, Simpson AJ, Mitchell TJ, Buttle DJ, Cross SS, Ince PG, Hellewell PG, Whyte MKB, Dockrell DH. Reactive oxygen species regulate neutrophil recruitment and survival in pneumococcal pneumonia. Am J Respir Crit Care Med. 2008;177(8):887-95.
11. Cieutat AM, Lobel P, August JT, Kjeldsen L, Sengelov H, Borregaard N, Bainton DF. Azurophilic granules of human neutrophilic leukocytes are deficient in lysosome-associated membrane proteins but retain the mannose 6-phosphate recognition marker. Blood. 1998;91(3):1044-58.

12. Brinkmann V, Reichard U, Goosmann C, Fauler B, Uhlemann Y, Weiss DS, Weinrauch Y, Zychlinsky A. Neutrophil extracellular traps kill bacteria. Science. 2004;303(5663):1532-5.
13. Geissmann F, Jung S, Littman DR. Blood monocytes consist of two principal subsets with distinct migratory properties. Immunity. 2003;19(1):71-82.
14. Yang J, Zhang L, Yu C, Yang XF, Wang H. Monocyte and macrophage differentiation: circulation inflammatory monocyte as biomarker for inflammatory diseases. Biomark Res. 2014;2(1):1.
15. Mandell LA, Wunderink RG, Anzueto A, Bartlett JG, Campbell GD, Dean NC, Dowell SF, File TM, Jr, Musher DM Niederman MS, Torres A, Whitney CG. Infectious Diseases Society of America/American Thoracic Society Consensus Guidelines on the Management of Community-Acquired Pneumonia in Adults. Clinical Infectious Diseases. 2007;44(Supplement_2):S27-S72.
16. Lim WS, Baudouin SV, George RC, Hill AT, Jamieson C, Le Jeune I, Macfarlane JT, Read PC, Roberts HJ, Levy ML, Wani M, Woodhead MA. BTS guidelines for the management of community acquired pneumonia in adults: update 2009. Thorax. 2009;64 Suppl 3:iii1-55.
17. Lee JS, Giesler DL, Gellad WF, Fine MJ. Antibiotic Therapy for Adults Hospitalized With Community-Acquired Pneumonia: A Systematic Review. JAMA. 2016;315(6):593-602.
18. Mongardon N, Max A, Bougle A, Pene F, Lemiale V, Charpentier J, Cariou A, Chiche JD, Bedos JP, Mira JP. Epidemiology and outcome of severe pneumococcal pneumonia admitted to intensive care unit: a multicenter study. Crit Care. 2012;16(4):R155.
19. Davidson AC, Banham S, Elliott M, Kennedy D, Gelder C, Glossop A, Church AC, Creagh-Brown B, Dodd JW, Felton T, Foëx B, Mansfield L, McDonnell, Parker R, Patterson CM, Sovani M, Thomas L. BTS/ICS guideline for the ventilatory management of acute hypercapnic respiratory failure in adults. Thorax. 2016;71 Suppl 2:ii1-35.
20. Slutsky AS. Mechanical ventilation. American College of Chest Physicians' Consensus Conference. Chest. 1993;104(6):1833-59.
21. Nash G, Blennerhassett J, Pontoppidan H. Pulmonary lesions associated with oxygen therapy and artificial ventilation. Laval Med. 1968;39(1):59-64.

22. Bellani G, Laffey JG, Pham T, Fan E, Brochard L, Esteban A, Gattinoni L, van Haren F, Larsson A, McAuley DF, Ranieri M, Rubenfeld G, Taylor Thompson B, Wrigge H, Slutsky AS, Pesenti A. LUNG SAFE Investigators; ESICM Trials Group. Epidemiology, Patterns of Care, and Mortality for Patients With Acute Respiratory Distress Syndrome in Intensive Care Units in 50 Countries. JAMA. 2016;315(8):788-800.
23. Wolthuis EK, Vlaar AP, Choi G, Roelofs JJ, Juffermans NP, Schultz MJ. Mechanical ventilation using non-injurious ventilation settings causes lung injury in the absence of pre-existing lung injury in healthy mice. Crit Care. 2009;13(1):R1.
24. Dreyfuss D, Soler P, Basset G, Saumon G. High inflation pressure pulmonary edema. Respective effects of high airway pressure, high tidal volume, and positive end-expiratory pressure. Am Rev Respir Dis. 1988;137(5):1159-64.
25. Bates JHT, Smith BJ. Ventilator-induced lung injury and lung mechanics. Ann Transl Med. 2018;6(19):378.
26. Kay SS, Bilek AM, Dee KC, Gaver DP, 3rd. Pressure gradient, not exposure duration, determines the extent of epithelial cell damage in a model of pulmonary airway reopening. J Appl Physiol (1985). 2004;97(1):269-76.
27. Tremblay L, Valenza F, Ribeiro SP, Li J, Slutsky AS. Injurious ventilatory strategies increase cytokines and c-fos m-RNA expression in an isolated rat lung model. The Journal of clinical investigation. 1997;99(5):944-52.
28. Ranieri VM, Suter PM, Tortorella C, De Tullio R, Dayer JM, Brienza A, Bruno F, Slutsky AS. Effect of mechanical ventilation on inflammatory mediators in patients with acute respiratory distress syndrome: a randomized controlled trial. JAMA. 1999;282(1):54-61.
29. Maniatis NA, Kardara M, Hecimovich D, Letsiou E, Castellon M, Roussos C, Shinin V, Votta-Vellis EG, Schwartz DE, Minshall RD. Role of caveolin-1 expression in the pathogenesis of pulmonary edema in ventilator-induced lung injury. Pulm Circ. 2012;2(4):452-60.
30. Imai Y, Parodo J, Kajikawa O, de Perrot M, Fischer S, Edwards V, Cutz E, Liu M, Keshavjee S, Martin TR, Marshall JC, Ranieri VM, Slutsky AS. Injurious mechanical ventilation and end-organ epithelial cell apoptosis and organ dysfunction in an experimental model of acute respiratory distress syndrome. JAMA. 2003;289(16):2104-12.

31. Slutsky AS, Ranieri VM. Ventilator-induced lung injury. N Engl J Med. 2013;369(22):2126-36.
32. Dhanireddy S, Altemeier WA, Matute-Bello G, O'Mahony DS, Glenny RW, Martin TR, Conrad Liles W. Mechanical ventilation induces inflammation, lung injury, and extra-pulmonary organ dysfunction in experimental pneumonia. Lab Invest. 2006;86(8):790-9.
33. Müller-Redetzky HC, Will D, Hellwig K, Kummer W, Tschernig T, Pfeil U, Paddenberg R, Menger MD, Kershaw O, Gruber AD, Weissman N, Hippenstiel S, Suttorp N, Witzenrath M. Mechanical ventilation drives pneumococcal pneumonia into lung injury and sepsis in mice: protection by adrenomedullin. Crit Care. 2014;18(2):R73-R.
34. Frank JA, Pittet JF, Wray C, Matthay MA. Protection from experimental ventilator-induced acute lung injury by IL-1 receptor blockade. Thorax. 2008;63(2):147-53.
35. Joshi H, Morley SC. Cells under stress: The mechanical environment shapes inflammasome responses to danger signals. J Leukoc Biol. 2019;106(1):119-25.
36. Kuipers MT, van der Poll T, Schultz MJ, Wieland CW. Bench-to-bedside review: Damage-associated molecular patterns in the onset of ventilator-induced lung injury. Crit Care. 2011;15(6):235.
37. Held HD, Boettcher S, Hamann L, Uhlig S. Ventilation-induced chemokine and cytokine release is associated with activation of nuclear factor-kappaB and is blocked by steroids. Am J Respir Crit Care Med. 2001;163(3 Pt 1):711-6.
38. B Moore B, Lawson WE, Oury TD, Sisson TH, Raghavendran K, Hogaboam CM. Animal models of fibrotic lung disease. Am J Respir Cell Mol Biol. 2013;49(2):167-79.
39. Kuipers MT, Aslami H, Janczy JR, van der Sluijs KF, Vlaar AP, Wolthuis EK, Choi G, Roelofs JJTH, Flavell RA, Sutterwala FS, Bresser P, Leemans JC, van der Poll T, Schultz MJ, Wieland CW. Ventilator-induced lung injury is mediated by the NLRP3 inflammasome. Anesthesiology. 2012;116(5):1104-15.
40. Chen Q, Zhou J, Zhang B, Chen Z, Luo Q, Song G. Cyclic Stretching Exacerbates Tendinitis by Enhancing NLRP3 Inflammasome Activity via F-Actin Depolymerization. Inflammation. 2018;41(5):1731-43.

41. Fang M, Fan S, Yao X, Liu N, Gao J, Wang Z, Xu T, Xian X, Li W. Transfection of Sox11 plasmid alleviates ventilator-induced lung injury via Sox11 and FAK. Biochem Biophys Res Commun. 2019;512(2):182-8.
42. Dunn I, Pugin J. Mechanical ventilation of various human lung cells in vitro: identification of the macrophage as the main producer of inflammatory mediators. Chest. 1999;116(1 Suppl):95s-7s.
43. Frank JA, Wray CM, McAuley DF, Schwendener R, Matthay MA. Alveolar macrophages contribute to alveolar barrier dysfunction in ventilator-induced lung injury. Am J Physiol Lung Cell Mol Physiol. 2006;291(6):L1191-8.
44. Li LF, Yu L, Quinn DA. Ventilation-induced neutrophil infiltration depends on c-Jun N-terminal kinase. Am J Respir Crit Care Med. 2004;169(4):518-24.
45. Belperio JA, Keane MP, Burdick MD, Londhe V, Xue YY, Li K, Phillips RJ, Strieter RM. Critical role for CXCR2 and CXCR2 ligands during the pathogenesis of ventilator-induced lung injury. J Clin Invest. 2002;110(11):1703-16.
46. Kooy NW, Royall JA, Ye YZ, Kelly DR, Beckman JS. Evidence for in vivo peroxynitrite production in human acute lung injury. Am J Respir Crit Care Med. 1995;151(4):1250-4.
47. Murphy DB, Cregg N, Tremblay L, Engelberts D, Laffey JG, Slutsky AS, Romaschin A, Kavanagh BP. Adverse ventilatory strategy causes pulmonary-to-systemic translocation of endotoxin. Am J Respir Crit Care Med. 2000;162(1):27-33.
48. dos Santos CC, Zhang H, Slutsky AS. From bench to bedside: bacterial growth and cytokines. Crit Care. 2002;6(1):4-6.
49. Morton SE, Knopp JL, Chase JG, Moller K, Docherty P, Shaw GM, Tawhai M. Predictive Virtual Patient Modelling of Mechanical Ventilation: Impact of Recruitment Function. Ann Biomed Eng. 2019;47(7):1626-41.
50. Brower RG, Matthay MA, Morris A, Schoenfeld D, Thompson BT, Wheeler A. Ventilation with lower tidal volumes as compared with traditional tidal volumes for acute lung injury and the acute respiratory distress syndrome. N Engl J Med. 2000;342(18):1301-8.
51. McAuley DF, Cross LM, Hamid U, Gardner E, Elborn JS, Cullen KM, Dushianthan A, Grocott MP, Matthay MA, O'Kane CM. Keratinocyte growth factor for the treatment of the acute respiratory distress syndrome (KARE): a randomised, double-blind, placebo-controlled phase 2 trial. Lancet Respir Med. 2017;5(6):484-91.

52. Bellingan G, Maksimow M, Howell DC, Stotz M, Beale R, Beatty M, Walsh T, Binning A, Davidson A, Kuper M, Shah S, Cooper J, Waris M, Yegutkin GG, Jalkanen J, Salmi M, Piippo I, Jalkanen M, Montgomery H, Jalkanen S. The effect of intravenous interferon-beta-1a (FP-1201) on lung CD73 expression and on acute respiratory distress syndrome mortality: an open-label study. Lancet Respir Med. 2014;2(2):98-107.
53. George PM, Wort SJ, Mitchell JA. Use of interferon beta for acute respiratory distress syndrome: proceed with caution. Lancet Respir Med. 2014;2(4):e2.
54. Kellum JA, Kong L, Fink MP, Weissfeld LA, Yealy DM, Pinsky MR, Fine J, Krichevsky A, Delude RL, Angus DC, GenIMS Investigators. Understanding the inflammatory cytokine response in pneumonia and sepsis: results of the Genetic and Inflammatory Markers of Sepsis (GenIMS) Study. Arch Intern Med. 2007;167(15):1655-63.
55. Calfee CS, Delucchi K, Parsons PE, Thompson BT, Ware LB, Matthay MA, NHLBI ARDS Network. Subphenotypes in acute respiratory distress syndrome: latent class analysis of data from two randomised controlled trials. Lancet Respir Med. 2014;2(8):611-20.
56. Novack V, Eisinger M, Frenkel A, Terblanche M, Adhikari NK, Douvdevani A, Amichay D, Almog Y. The effects of statin therapy on inflammatory cytokines in patients with bacterial infections: a randomized double-blind placebo controlled clinical trial. Intensive Care Med. 2009;35(7):1255-60.
57. Müller HC, Hellwig K, Rosseau S, Tschernig T, Schmiedl A, Gutbier B, Schmeck B, Hippenstiel S, Peters H, Morawietz L, Suttorp N, Witzenrath M. Simvastatin attenuates ventilator-induced lung injury in mice. Crit Care. 2010;14(4):R143.
58. Makris D, Manoulakas E, Komnos A, Papakrivou E, Tzovaras N, Hovas A, Zintzaras E, Zakynthinos E. Effect of pravastatin on the frequency of ventilator-associated pneumonia and on intensive care unit mortality: open-label, randomized study. Crit Care Med. 2011;39(11):2440-6.
59. Papazian L, Roch A, Charles PE, Penot-Ragon C, Perrin G, Roulier P, Goutorbe P, Lefrant JY, Wiramus S, Jung B, Perbet S, Hernu R, Nau A, Baldesi O, Allardet-Servent J, Baumstarck K, Jouve E, Moussa M, Hraiech S, Guervilly C, Forel JM, STATIN-VAP Study Group. Effect of statin therapy on mortality in patients with

ventilator-associated pneumonia: a randomized clinical trial. JAMA. 2013;310(16):1692-700.
60. Ehrenstein MR, Notley CA. The importance of natural IgM: scavenger, protector and regulator. Nat Rev Immunol. 2010;10(11):778-86.
61. Boes M. Role of natural and immune IgM antibodies in immune responses. Mol Immunol. 2000;37(18):1141-9.
62. Fleming SD. Naturally occurring autoantibodies mediate ischemia/reperfusion-induced tissue injury. Adv Exp Med Biol. 2012;750:174-85.
63. Woof JM, Kerr MA. The function of immunoglobulin A in immunity. J Pathol. 2006;208(2):270-82.
64. Seely AJ, Naud JF, Campisi G, Giannias B, Liu S, DiCarlo A, Ferri LE, Pascual JL, Tchervenkov J, Christou NV. Alteration of chemoattractant receptor expression regulates human neutrophil chemotaxis in vivo. Ann Surg. 2002;235(4):550-9.
65. Taccone FS, Stordeur P, De Backer D, Creteur J, Vincent JL. Gamma-globulin levels in patients with community-acquired septic shock. Shock. 2009;32(4):379-85.
66. Ichiyama T, Yoshitomi T, Nishikawa M, Fujiwara M, Matsubara T, Hayashi T, Furukawa S. NF-kappaB activation in peripheral blood monocytes/macrophages and T cells during acute Kawasaki disease. Clin Immunol. 2001;99(3):373-7.
67. Aukrust P, Müller F, Svenson M, Nordøy I, Bendtzen K, Frøland SS. Administration of intravenous immunoglobulin (IVIG) in vivo--down-regulatory effects on the IL-1 system. Clin Exp Immunol. 1999;115(1):136-43.
68. Menezes MCS, Benard G, Sato MN, Hong MA, Duarte AJS. In vitro Inhibitory Activity of Tumor Necrosis Factor Alpha and Interleukin-2 of Human Immunoglobulin Preparations. International Archives of Allergy and Immunology. 1997;114(4):323-8.
69. Kreymann KG, de Heer G, Nierhaus A, Kluge S. Use of polyclonal immunoglobulins as adjunctive therapy for sepsis or septic shock. Crit Care Med. 2007;35(12):2677-85.
70. Alejandria MM, Lansang MA, Dans LF, Mantaring JB, 3rd. Intravenous immunoglobulin for treating sepsis, severe sepsis and septic shock. Cochrane Database Syst Rev. 2013(9):CD001090.
71. Vonarburg C, Loetscher M, Spycher MO, Kropf A, Illi M, Salmon S, Roberts S, Steinfuehrer K, Campbell I, Koernig S, Bain J, Edler M, Baumann U, Miescher S, Metzger DW, Schaub A, Käsermann F, Zuercher AW. Topical application of

nebulized human IgG, IgA and IgAM in the lungs of rats and non-human primates. Respir Res. 2019;20(1):99.
72. Werdan K, Pilz G, Bujdoso O, Fraunberger P, Neeser G, Schmieder RE, Viell B, Marget W, Seewald M, Walger P, Stuttmann R, Speichermann N, Peckelsen C, Kurowski V, Osterhues HH, Verner L, Neumann R, Müller-Werdan U, Score-Based Immunoglobulin Therapy of Sepsis (SBITS) Study Group. Score-based immunoglobulin G therapy of patients with sepsis: the SBITS study. Crit Care Med. 2007;35(12):2693-701.
73. Welte T, Dellinger RP, Ebelt H, Ferrer M, Opal SM, Singer M, Vincent JL, Werdan K, Martin-Loeches I, Almirall J, Artigas A, Ayestarán JI, Nuding S, Ferrer R, Rodrígues GS, Shankar-Hari M, Álvarez-Lerma F, Riessen R, Sirvent JM, Kluge S, Zacharowski K, Mora JB, Lapp H, Wöbker G, Achtzehn U, Brealey D, Kempa A, García MS, Brederlau J, Kochanek M, Reschreiter HP, Wise MP, Belohradsky BH, Bobenhausen I, Dälken B, Dubovy P, Langohr P, Mayer M, Schuttrümpf J, Wartenberg-Demand A, Wippermann U, Wolf D, Torres A. Efficacy and safety of trimodulin, a novel polyclonal antibody preparation, in patients with severe community-acquired pneumonia: a randomized, placebo-controlled, double-blind, multicenter, phase II trial (CIGMA study). Intensive Care Med. 2018;44(4):438-48.
74. Cui J, Wei X, Lv H, Li Y, Li P, Chen Z, Liu G. The clinical efficacy of intravenous IgM-enriched immunoglobulin (pentaglobin) in sepsis or septic shock: a meta-analysis with trial sequential analysis. Ann Intensive Care. 2019;9(1):27.
75. Shankar-Hari M, Spencer J, Sewell WA, Rowan KM, Singer M. Bench-to-bedside review: Immunoglobulin therapy for sepsis - biological plausibility from a critical care perspective. Crit Care. 2012;16(2):206.
76. Dames C, Akyuz L, Reppe K, Tabeling C, Dietert K, Kershaw O, Gruber AD, Meisel C, Meisel C, Witzenrath M, Engel O. Miniaturized bronchoscopy enables unilateral investigation, application, and sampling in mice. Am J Respir Cell Mol Biol. 2014;51(6):730-7.
77. Lachmann RA, van Kaam AH, Haitsma JJ, Verbrugge SJ, Delreu F, Lachmann B. Immunoglobulin M-enriched intravenous polyclonal immunoglobulins reduce bacteremia following Klebsiella pneumoniae infection in an acute respiratory distress syndrome rat model. Exp Lung Res. 2004;30(4):251-60.
78. Whitehead T, Slutsky AS. The pulmonary physician in critical care * 7: ventilator induced lung injury. Thorax. 2002;57(7):635-42.

79. Ricard JD, Dreyfuss D, Saumon G. Ventilator-induced lung injury. Eur Respir J Suppl. 2003;42:2s-9s.
80. Berger S, Goekeri C, Gupta SK, Vera J, Dietert K, Behrendt U, Lienau J, Wienhold SM, Gruber AD, Suttorp N, Witzenrath M, Nouailles G. Delay in antibiotic therapy results in fatal disease outcome in murine pneumococcal pneumonia. Crit Care. 2018;22(1):287.
81. Vaschetto R, Clemente N, Pagni A, Esposito T, Longhini F, Mercalli F, Boggio E, Boldorini R, Ciocchetti A, Dianzai U, Navalesi P. A double blind randomized experimental study on the use of IgM-enriched polyclonal immunoglobulins in an animal model of pneumonia developing shock. Immunobiology. 2017;222(12):1074-80.
82. Barratt-Due A, Sokolov A, Gustavsen A, Hellerud BC, Egge K, Pischke SE, Lindstad JK, Pharo A, Castellheim A, Thorgersen EB, Mollnes TE. Polyvalent immunoglobulin significantly attenuated the formation of IL-1β in Escherichia coli-induced sepsis in pigs. Immunobiology. 2013;218(5):683-9.
83. Kozicky LK, Zhao ZY, Menzies SC, Fidanza M, Reid GS, Wilhelmsen K, Hellman J, Hotte N, Madsen K, Sly LM. Intravenous immunoglobulin skews macrophages to an anti-inflammatory, IL-10-producing activation state. J Leukoc Biol. 2015;98(6):983-94.
84. Shmygalev S, Damm M, Knels L, Strassburg A, Wünsche K, Dumke R, Stehr SN, Koch T, Heller AR. IgM-enriched solution BT086 improves host defense capacity and energy store preservation in a rabbit model of endotoxemia. Acta Anaesthesiol Scand. 2016;60(4):502-12.
85. Rieben R, Roos A, Muizert Y, Tinguely C, Gerritsen AF, Daha MR. Immunoglobulin M-enriched human intravenous immunoglobulin prevents complement activation in vitro and in vivo in a rat model of acute inflammation. Blood. 1999;93(3):942-51.
86. Nimmerjahn F, Ravetch JV. Anti-Inflammatory Actions of Intravenous Immunoglobulin. Annual Review of Immunology. 2008;26(1):513-33.
87. Xu C, Poirier B, Duong Van Huyen JP, Lucchiari N, Michel O, Chevalier J, Kaveri S. Modulation of endothelial cell function by normal polyspecific human intravenous immunoglobulins: a possible mechanism of action in vascular diseases. Am J Pathol. 1998;153(4):1257-66.

88. Rittirsch D, Flierl MA, Nadeau BA, Day DE, Huber-Lang M, Mackay CR, Zetoune FS, Gerard NP, Cianflone K, Köhl J, Gerard C, Sarma JV, Ward PA. Functional roles for C5a receptors in sepsis. Nat Med. 2008;14(5):551-7.
89. Hagiwara S, Iwasaka H, Hasegawa A, Asai N, Noguchi T. High-dose intravenous immunoglobulin G improves systemic inflammation in a rat model of CLP-induced sepsis. Intensive Care Med. 2008;34(10):1812-9.
90. Michalick L, Erfinanda L, Weichelt U, van der Giet M, Liedtke W, Kuebler WM. Transient Receptor Potential Vanilloid 4 and Serum Glucocorticoid-regulated Kinase 1 Are Critical Mediators of Lung Injury in Overventilated Mice In Vivo. Anesthesiology. 2017;126(2):300-11.
91. Baxendale HE, Johnson M, Stephens RCM, Yuste J, Klein N, Brown JS, Goldblatt D. Natural human antibodies to pneumococcus have distinctive molecular characteristics and protect against pneumococcal disease. Clin Exp Immunol. 2008;151(1):51-60.

11. Statutory Declaration

“I, Alexander Taylor by personally signing this document in lieu of an oath, hereby affirm that I prepared the submitted dissertation on the topic “Experimental investigation of a novel immunoglobulin-based adjuvant therapy for severe pneumonia under mechanical ventilation” (“Experimentelle Untersuchung einer neuartigen adjuvanten Therapie auf Immunglobulinbasis bei schwerer Lungenentzündung unter mechanischer Beatmung”), independently and without the support of third parties, and that I used no other sources and aids than those stated.

All parts which are based on the publications or presentations of other authors, either in letter or in spirit, are specified as such in accordance with the citing guidelines. The sections on methodology (in particular regarding practical work, laboratory regulations, statistical processing) and results (in particular regarding figures, charts and tables) are exclusively my responsibility.

Furthermore, I declare that I have correctly marked all of the data, the analyses, and the conclusions generated from data obtained in collaboration with other persons, and that I have correctly marked my own contribution and the contributions of other persons (cf. declaration of contribution). I have correctly marked all texts or parts of texts that were generated in collaboration with other persons.

My contributions to any publications to this dissertation correspond to those stated in the below joint declaration made together with the supervisor. All publications created within the scope of the dissertation comply with the guidelines of the ICMJE (International Committee of Medical Journal Editors; www.icmje.org) on authorship. In addition, I declare that I shall comply with the regulations of Charité – Universitätsmedizin Berlin on ensuring good scientific practice.

I declare that I have not yet submitted this dissertation in identical or similar form to another Faculty.

The significance of this statutory declaration and the consequences of a false statutory declaration under criminal law (Sections 156, 161 of the German Criminal Code) are known to me.”

Date 01.03.2021 Signature A. Taylor

12. Curriculum vitae

My curriculum vitae does not appear in the electronic version of my paper for reasons of data protection.

My curriculum vitae does not appear in the electronic version of my paper for reasons of data protection.

13. Acknowledgements

There are many people to whom I owe a great debt of gratitude but two in particular stand out. Firstly, I would like to express both my great admiration and thanks to Prof. Martin Witzenrath. He offered me this opportunity not only to undertake this piece of research in his working group but also has supported my career both scientifically and in the medical domain. The quality of work produced by his laboratory speaks for itself but that is only half the story of the dynamic approach he takes to the research. In many ways he took a chance on me and I will be eternally grateful for everything he has done for me.

Secondly, but by no means less, I thank my supervisor, Dr. Geraldine Nouailles-Kursar. She is a formidable scientist, constantly challenging her students to excel but at the same time providing a nurturing environment personally, especially in difficult times. I have no doubt she is destined for something special in her field and it has been an absolute joy to work with her.

Equally Dr. Sandra Wienhold was an ever-present source of wisdom and helped guide me through some more challenging aspects of the experiment, despite also having to look after her own students! Ulrike Behrendt is the technical backbone of the group and has smoothly navigated me through no end of sticky experimental situations. Also, I must thank Dr. Jasmin Lienau for going over my thesis with a fine-tooth comb!

I would like to thank everyone in the laboratory, but certain members deserve special mention for their further support: Verena Stössel, Kevin Braun, Dr. Luiz Gustavo Teixeira Alves, Dr. Birgitt Gutbier, Dr. Katrin Reppe, Dr. Matthias Felten, Dr. Cengiz Gökeri, Markus Brack, Kerstin Linke, Chunjiang Tan and Yawen Liu. Thank you.

I must also thank Biotest AG for providing biological material and their technical support to facilitate this project. Similarly, I am hugely grateful to the Jürgen Manchot Stiftung for their financial support, that has allowed me to pursue my scientific endeavors.

Finally, I must spare a mention for two sets of families. Firstly, my own, who have supported me unquestionably despite upping sticks and moving to Germany and then also the family of my partner (now fiancée!) who have welcomed me with open arms to a new home. Lastly but absolutely not least, I must extend my deepest thanks to my fiancée Nora. She is my constant inspiration and strength, and she provides me with untold support behind closed doors, without which I would not be able to succeed.

14. Confirmation by a statistician

CHARITÉ

CharitéCentrum für Human- und Gesundheitswissenschaften

Charité | Campus Charité Mitte | 10117 Berlin

Institut für Biometrie und klinische Epidemiologie (iBikE)

Direktor: Prof. Dr. Geraldine Rauch

Postantschrift:
Charitéplatz 1 | 10117 Berlin
Besucheranschrift:
Reinhardtstr. 58 | 10117 Berlin

Tel. +49 (0)30 450 562171
geraldine.rauch@charite.de
https://biometrie.charite.de/

Name, Vorname: Taylor, Alexander

Emailadresse: alexander.taylor@charite.de

Matrikelnummer:

PromotionsbetreuerIn: Prof. Dr. med. Martin Witzenrath

Promotionsinstitution / Klinik: Medizinische Klinik mit Schwerpunkt Infektiologie und Pneumologie

Bescheinigung

Hiermit bescheinige ich, dass Herr Alexander Taylor innerhalb der Service Unit Biometrie des Instituts für Biometrie und klinische Epidemiologie (iBikE) bei mir eine statistische Beratung zu einem Promotionsvorhaben wahrgenommen hat. Folgende Beratungstermine wurden wahrgenommen:

- Termin 1: *03.02.2021*

Folgende wesentliche Ratschläge hinsichtlich einer sinnvollen Auswertung und Interpretation der Daten wurden während der Beratung erteilt:

- Für eine ANOVA sind normalverteilte Daten notwendig. Für ordinale Daten sind andere Verfahren angezeigt, wie z.B. Pearson's Chi-square test.
- Eine Fallzahlplanung zur Absicherung der statistischen Power ist im Rahmen der Versuchsplanung sinnvoll.

Diese Bescheinigung garantiert nicht die richtige Umsetzung der in der Beratung gemachten Vorschläge, die korrekte Durchführung der empfohlenen statistischen Verfahren und die richtige Darstellung und Interpretation der Ergebnisse. Die Verantwortung hierfür obliegt allein dem Promovierenden. Das Institut für Biometrie und klinische Epidemiologie übernimmt hierfür keine Haftung.

Datum: 04.02.2021 Name des Beraters: Maximilian Wechsung